CANADIAN THESES ON MICROFICHE

I.S.B.N.

THESES CANADIENNES SUR MICROFICHE

National Library of Canada
Collections Development Branch

Canadian Theses on
Microfiche Service

Ottawa, Canada
K1A 0N4

Bibliothèque nationale du Canada
Direction du développement des collections

Service des thèses canadiennes
sur microfiche

## NOTICE

The quality of this microfiche is heavily dependent upon the quality of the original thesis submitted for microfilming. Every effort has been made to ensure the highest quality of reproduction possible.

If pages are missing, contact the university which granted the degree.

Some pages may have indistinct print especially if the original pages were typed with a poor typewriter ribbon or if the university sent us a poor photocopy.

Previously copyrighted materials (journal articles, published tests, etc.) are not filmed.

Reproduction in full or in part of this film is governed by the Canadian Copyright Act, R.S.C. 1970, c. C-30. Please read the authorization forms which accompany this thesis.

THIS DISSERTATION
HAS BEEN MICROFILMED
EXACTLY AS RECEIVED

## AVIS

La qualité de cette microfiche dépend grandement de la qualité de la thèse soumise au microfilmage. Nous avons tout fait pour assurer une qualité supérieure de reproduction.

S'il manque des pages, veuillez communiquer avec l'université qui a conféré le grade.

La qualité d'impression de certaines pages peut laisser à désirer, surtout si les pages originales ont été dactylographiées à l'aide d'un ruban usé ou si l'université nous a fait parvenir une photocopie de mauvaise qualité.

Les documents qui font déjà l'objet d'un droit d'auteur (articles de revue, examens publiés, etc.) ne sont pas microfilmés.

La reproduction, même partielle, de ce microfilm est soumise à la Loi canadienne sur le droit d'auteur, SRC 1970, c. C-30. Veuillez prendre connaissance des formules d'autorisation qui accompagnent cette thèse.

LA THÈSE A ÉTÉ
MICROFILMÉE TELLE QUE
NOUS L'AVONS REÇUE

NL-339 (r. 82/08)

Canada

178

0-315-12491-1

National Library of Canada | Bibliothèque nationale du Canada

Canadian Theses Division | Division des thèses canadiennes

Ottawa, Canada
K1A 0N4

60402

## PERMISSION TO MICROFILM — AUTORISATION DE MICROFILMER

• Please print or type — Écrire en lettres moulées ou dactylographier

Full Name of Author — Nom complet de l'auteur

MOSTAFA SHAHRIAR

| Date of Birth — Date de naissance | Country of Birth — Lieu de naissance |
|---|---|
| NOV 28, 1953 | BANGLADESH |

Permanent Address — Résidence fixe

CHITTAGONG UNIV. BANGLADESH

Title of Thesis — Titre de la thèse

~~INTERPRETATION OF~~ REFRACTION DATA FROM SOUTHERN SASKATCHEWAN: A DETAILED INTERPRETATION OF THE 1979 EAST-WEST $CO_2$-CRUST PROFILE

University — Université

U OF A.

Degree for which thesis was presented — Grade pour lequel cette thèse fut présentée

M. Sc.

| Year this degree conferred — Année d'obtention de ce grade | Name of Supervisor — Nom du directeur de thèse |
|---|---|
| 1982 | G. L. CUMMING. |

Permission is hereby granted to the NATIONAL LIBRARY OF CANADA to microfilm this thesis and to lend or sell copies of the film.

The author reserves other publication rights, and neither the thesis nor extensive extracts from it may be printed or otherwise reproduced without the author's written permission.

L'autorisation est, par la présente, accordée à la BIBLIOTHÈQUE NATIONALE DU CANADA de microfilmer cette thèse et de prêter ou de vendre des exemplaires du film.

L'auteur se réserve les autres droits de publication; ni la thèse ni de longs extraits de celle-ci ne doivent être imprimés ou autrement reproduits sans l'autorisation écrite de l'auteur.

| Date | Signature |
|---|---|
| OCT. 14, 82. | M. Shahriar |

NL-91 (4/77)

THE UNIVERSITY OF ALBERTA

# REFRACTION DATA FROM SOUTHERN SASKATCHEWAN: A DETAILED INTERPRETATION OF THE 1979 EAST-WEST COCRUST PROFILE

by

MOSTAFA SHAHRIAR

A THESIS

SUBMITTED TO THE FACULTY OF GRADUATE STUDIES AND RESEARCH

IN PARTIAL FULFILMENT OF THE REQUIREMENTS FOR THE DEGREE

OF MASTER OF SCIENCE

IN

GEOPHYSICS

DEPARTMENT OF PHYSICS

EDMONTON, ALBERTA

FALL, 1982

THE UNIVERSITY OF ALBERTA

**RELEASE FORM**

NAME OF AUTHOR MOSTAFA SHAHRIAR

TITLE OF THESIS REFRACTION DATA FROM SOUTHERN SASKATCHEWAN: A DETAILED INTERPRETATION OF THE 1979 EAST-WEST CO-CRUST PROFILE

DEGREE FOR WHICH THESIS WAS PRESENTED MASTER OF SCIENCE

YEAR THIS DEGREE GRANTED FALL, 1982

Permission is hereby granted to THE UNIVERSITY OF ALBERTA LIBRARY to reproduce single copies of this thesis and to lend or sell such copies for private, scholarly or scientific research purposes only.

The author reserves other publication rights, and neither the thesis nor extensive extracts from it may be printed or otherwise reproduced without the author's written permission.

(SIGNED) Mostafa

PERMANENT ADDRESS:

6094 Michael Park

Edmonton, Alta

T6H 5A1

DATED Oct 14 1982.

THE UNIVERSITY OF ALBERTA

FACULTY OF GRADUATE STUDIES AND RESEARCH

The undersigned certify that they have read, and recommend to the Faculty of Graduate Studies and Research, for acceptance, a thesis entitled REFRACTION DATA FROM SOUTHERN SASKATCHEWAN:A DETAILED INTERPRETATION OF THE 1979 EAST-WEST CO-CRUST PROFILE submitted by MOSTAFA SHAHRIAR in partial fulfilment of the requirements for the degree of MASTER OF SCIENCE in GEOPHYSICS.

.....G.h.Cumming.....

Supervisor

..E..R...Kanasewich...

.....D.A.Hegan.....

...R.A.Burwash.....

Date October 07, 1982.

## ABSTRACT

Detailed interpretation of the east-west profile of CO-CRUST 1979 refraction/wide angle reflection data has been carried out on the basis of horizontal layered model, WHB inversion, $T^2$-$X^2$ analysis and synthetic modelling. First and secondary arrivals were treated under the constraints of critical points and relative amplitudes to reach a suitable crustal model. Two low velocity zones were proposed in the upper and middle crust at depths of 11-14 km and 25-29 km which could be related to high conductivity materials in the crust. The depth of the Moho is approximately 44.5 km under the study area.

The profile lies entirely within the Churchill province and the model derived here appears to be a composite of the Swift Current-Suffield model of Chandra and Cumming (1972) and the model of Moon and de Landro (1981) which are on opposite ends of the profile under cosideration. A north-south crustal fault across the eastern section of the profile at a longitude somewhat east of 103°W may separate the profile area from the regions further east.

**ACKNOWLEDGEMENTS**

I wish to express my sincere thanks to Dr. G. L. Cumming whose guidance, work and encouragement have been invaluable throughout the entire programme.

Acknowledgement is also due to various faculty members and graduate students in Geophysics who have been very patient in discussing various topics related to this work.

Mr. Charles McCloughan is to be thanked for helping me during the preliminary processing work.

I am also grateful to the Department of Physycs, University of Alberta for supporting me with a graduate teaching assistantship during this study.

Finally my special thanks are due to the CO-CRUST 1979 group and other related persons who assisted in the field operation.

## Table of Contents


| Chapter | Page |
|---|---|
| 1. INTRODUCTION | 1 |
| 2. GEOLOGY AND GEOPHYSICS OF THE STUDY AREA | 4 |
| 2.1 General Geology: | 4 |
| 2.2 Gravity and Magnetic information: | 11 |
| 2.3 Previous seismic studies: | 14 |
| 3. DATA ACQUISITION & INSTRUMENTATION | 18 |
| 4. THEORETICAL CONSIDERATIONS | 21 |
| 4.1 On the use of some basic parameters: | 21 |
| 4.2 Apparent velocity: | 23 |
| 4.3 Calculation of Depth: | 24 |
| 4.4 Exact solution: | 27 |
| 4.5 $T^2$-$X^2$ method: | 28 |
| 4.6 Theoretical seismograms: | 30 |
| 4.7 Low velocity zones: | 32 |
| 5. DIGITAL PROCESSING | 34 |
| 5.1 Presentation of seismic records: | 34 |
| 5.2 Spectral analysis: | 36 |
| 5.3 Digital filtering: | 40 |
| 5.4 Correlation: | 42 |
| 6. RESULTS AND INTERPRETATION | 47 |
| 6.1 Horizontal layer model: | 47 |
| 6.2 WHB inversion: | 59 |
| 6.3 Analysis of reflection branches: | 61 |
| 6.4 Synthetic modelling: | 64 |
| 7. DISCUSSION | 74 |
| BIBLIOGRAPHY | 83 |

## List of Tables


| Table | | Page |
|---|---|---|
| 6.1 | Comparison of results from well logs and observed seismic data. | 56 |
| 6.2 | Calculated parameters for horizontal layer model (M1) from first arrivals. | 57 |
| 6.3 | Calculated model parameters from $T^2$-$X^2$ analysis. | 63 |
| 6.4 | Parameters for the final model (M4). | 68 |

## List of Figures


| Figure | | Page |
|---|---|---|
| 1.1 | Refraction profiles of the CO-CRUST 1979 experiment (modified from Kazmierczak, 1980). | 2 |
| 2.1 | Reference geological column for southern Saskatchewan indicating order of geological systems (arrows indicate major unconformities). | 5 |
| 2.2 | Map showing structural provinces in Canada (from Geology and Economic Minerals of Canada, 1970). | 7 |
| 2.3 | Basemap showing tectonic lineaments in the study area (modified from Sprenke, 1982). | 8 |
| 2.4 | Geology of the northern part of NACP anomaly (after Camfield and Gough, 1977). | 10 |
| 2.5 | Bouguer gravity anomaly of southern plains (after Lee, 1977). | 12 |
| 2.6 | Magnetic anomaly map covering eastern part of the study area (after Green et al., 1979). | 13 |
| 2.7 | Crustal models from previous refraction experiments in Manitoba, southern Saskatchewan and southern Alberta (after Kazmierczak, 1980). | 15 |
| 5.1 | Power spectrum for records at distances 12 and 31.5 km from the shot. | 38 |
| 5.2 | Power spectrum for records at distances 59 and 95 km from the shot. | 39 |
| 5.3 | Example showing frequency filtering using an eight pole Butterworth filter. | 41 |
| 5.4 | Vertical component seismogram of line-C from CO-CRUST 1979 refraction experiment (Filter 4-15 Hz Bessel). | 43 |
| 5.5 | Seismogram of line-C showing correlated reflection events from CO-CRUST 1979 refraction data (Filter 6-13 Hertz Butterworth). | 44 |
| 6.1 | Normalization of traces with respect to | |

Figure Page

the average noise level before the first arrivals. .....50

6.2 Normalization of traces keeping amplitudes of the prominent phases constant. .....51

6.3 Synthetic showing arrivals (PLR) from top of the low velocity layer in the basement. PC, PCR & PCR1 specify the refracted, reflected and multiple reflected branches from the sub-basement layer (after Braile & Smith, 1975). .....52

6.4 Correlated secondary arrivals corresponding to a possible layer of velocity 4.1 km/sec (filter 3.5-8.5 Hertz Butterworth). .....54

6.5 Model M1 from horizontal layer interpretation. .....58

6.6 Model M2 from WHB inversion. .....60

6.7 Model M3 from $T^2$-$X^2$ analysis. .....65

6.8 Synthetic seismogram obtained from model M1 of horizontal layer interpretation (a dot on the PmP indicates the position of the maximum amplitude). .....69

6.9 Synthetic seismogram from the final model M4 (a dot on the PmP indicates the position of the maximum amplitude). .....70

6.10 Final model (M4) showing the crustal stucture under the study area. .....71

6.11 Ray diagram corresponding to the final model (M4). Dashed curves represent the wave fronts. .....72

7.1 Crustal models from CO-CRUST 1979 refraction experiment (after Sprenke, 1982). .....80

7.2 Crustal model from CO-CRUST 1977 east-west refraction profile (after Moon and de Landro, 1981). .....81

# 1. INTRODUCTION

In recent years, determination of crustal velocity structure by means of explosion seismology has been a major objective of the Consortium for Crustal Reconnaissance Using Seismic Techniques (CO-CRUST). During the summer months of 1977, 1979 and 1981 this consortium conducted surveys in southern Manitoba, central and southern Saskatchewan. Near vertical reflection and refraction/wide angle reflection techniques were employed in these surveys. This study is a part of this integrated reconnaissance program and uses the refraction data for the interpretation of the east-west profile in southern Saskatchewan (line-C figure-1.1). Data for this profile were collected in 1979 from two different shots detonated from Limerick at the western end of the profile. The general aim of the study is to establish a reliable cross-section of the crustal lithosphere under the study area. The following three aspects will be emphasized throughout the study:

(1) establish a velocity depth function and compare it to the results obtained in southern Alberta and southern Manitoba from similar studies.

(2) look for any seismic expression of the conductive belt (see chapter-2) proposed by Camfield and Gough (1975) which crosses the same profile.

(3) detect the so called Riel discontinuity in the lower crust.

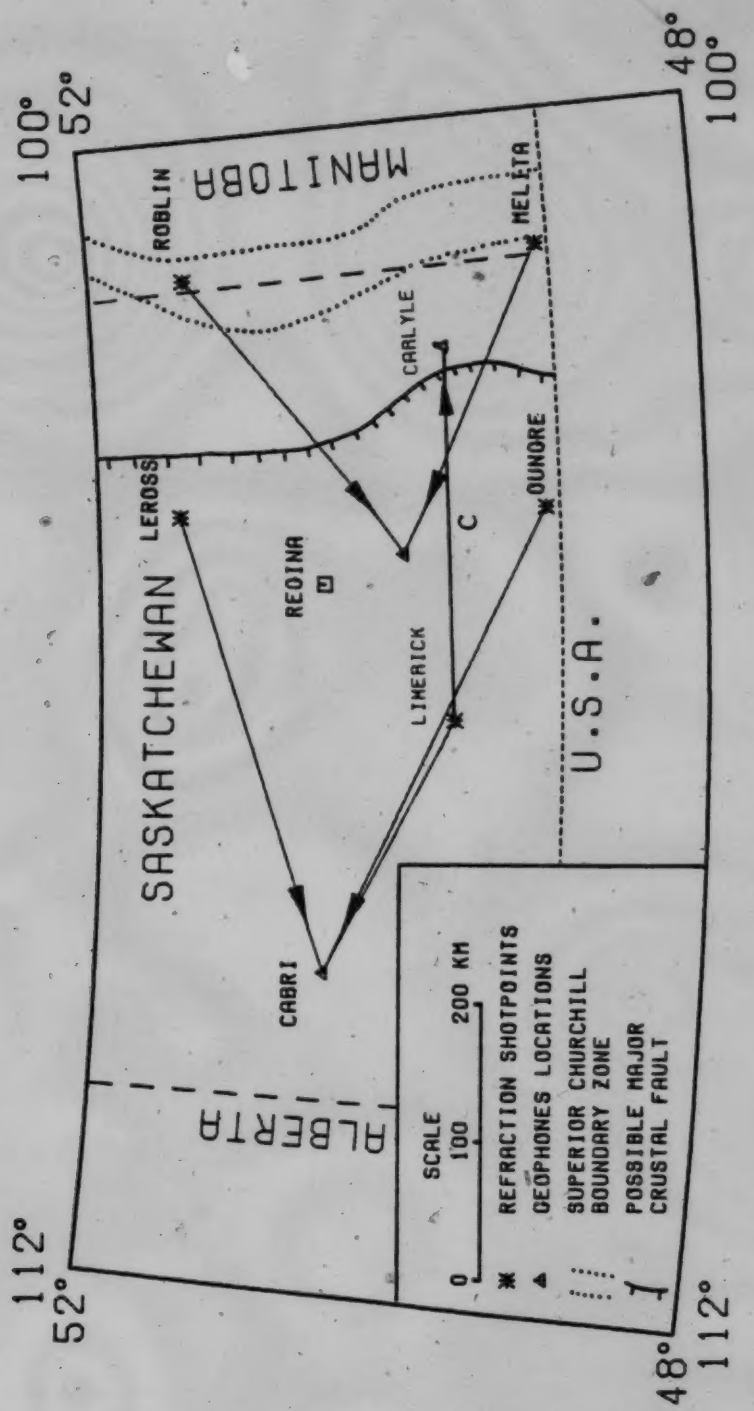


Figure 1.1 Refraction profiles of the CO-CRUST 1979 experiment (after Kazmierczak, 1980).

In chapter-2 we discuss background geology and geophysics of the study area. A description of data acquisition and field procedure has been included in chapter-3. Chapter-4 describes basic theories used to calculate crustal velocity and depth values including their upper and lower bounds. Chapter-5 deals with various steps involved in the systematic data processing. In chapter-6 calculated model parameters are interpreted in terms of different theories discussed in chapter-4. Finally a discussion of the derived crustal model in connection with different physical parameters such as lithology, conductivity and porosity etc is included in chapter-7.

## 2. GEOLOGY AND GEOPHYSICS OF THE STUDY AREA

### 2.1 General Geology:

The east-west profile of the CO-CRUST 1979 refraction experiment is located in the southern part of Saskatchewan. The landscape is essentially plain and constitutes the central part of the greater Interior Platform. Near surface sediments of Cretaceous age are essentially flat lying and have an average elevation of a few hundred meters above sea level. Older and gently rolling landscape has been burried by deposits of glacial till, sand and gravel. The Phanerozoic sedimentary section is up to 3.0 km thick near south-east Saskatchewan. The sediments thin northward to the exposed craton of northern Saskatchewan. This difference is due to varied basin subsidence and sedimentation in different regions. Subsidence was accentuated at various times throughout the Phanerozoic and basin sedimentation was locally affected by movements of structural regions or blocks of the Precambrian basement delimited by lineaments as well as by solution of massive halite beds of the Middle Devonian Praire Evaporite, which also resulted in the collapse of overlying strata. The base of the stratigraphic column is a succession of early Paleozoic clastics followed by Ordovician to Mississipian carbonate and evaporites and Jurassic to Pleistocene clastics (figure-2.1). The clastics of the Cambrian lie

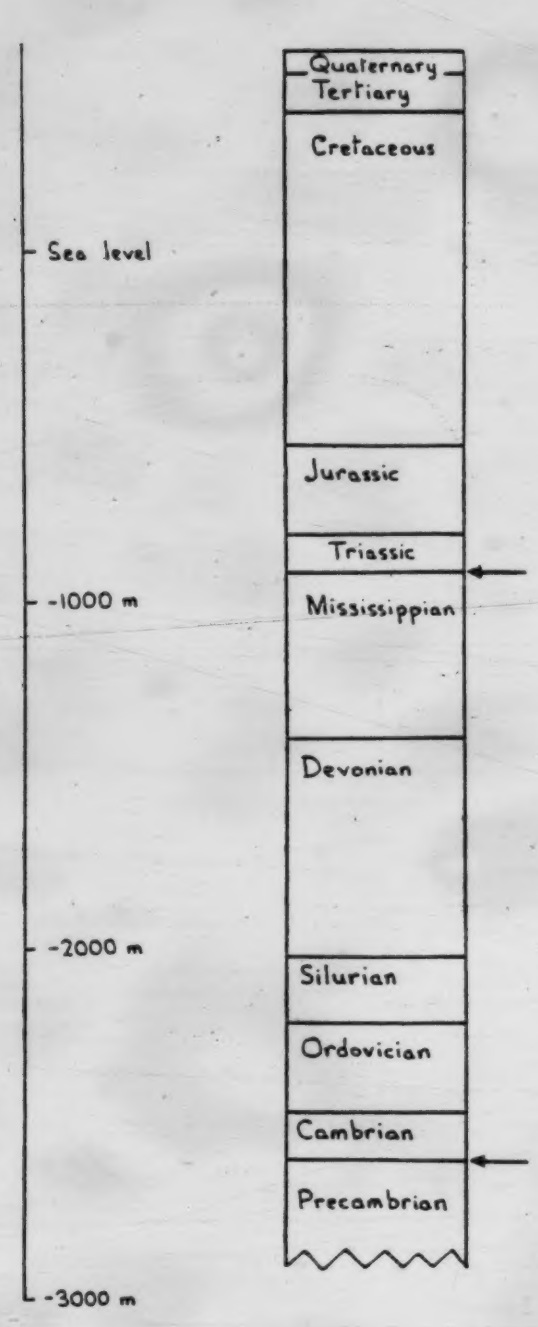


Figure 2.1 Reference geological column for southern Saskatchewan indicating order of geological systems (arrows indicate major unconformities).

unconformably on the basement.

Geologic information on the Precambrian comes from studies of the exposed shield (Bell, 1971) and studies from core samples (Burwash and Culbert, 1976). The basement under the Phanerozoic appears to be a south-westward continuation of the exposed Precambrian of the shield area. Its composition under the study area is basically metamorphosed and volcanic-plutonic rocks with weak or no trend, markedly differing from that of other geologic regions in Canada. In fact geophysical data and radiometric age determinations indicate that the Canadian Precambrian consists of a number of structural provinces (figure-2.2) having distinct geophysical signatures of their own.

The Superior province in the exposed shield of eastern Manitoba is Kenoran in age and is dominated by east-west trending structures of greenstone and gneissic belts, both rock complexes being extensively intruded by granitic plutons.

The Churchill province as exposed to the north consists mainly of metasediments and migmatites. Its rocks are of Hudsonian age and show variable trend directions. Large masses of weakly foliated granitic rocks are common. Among the regional assemblages near the study area are the Flin Flon belt, largely composed of Amisk-Missi metasedimentary-metavolcanic units and the Kisseynew belt, a gneissic terrain (figure-2.3).

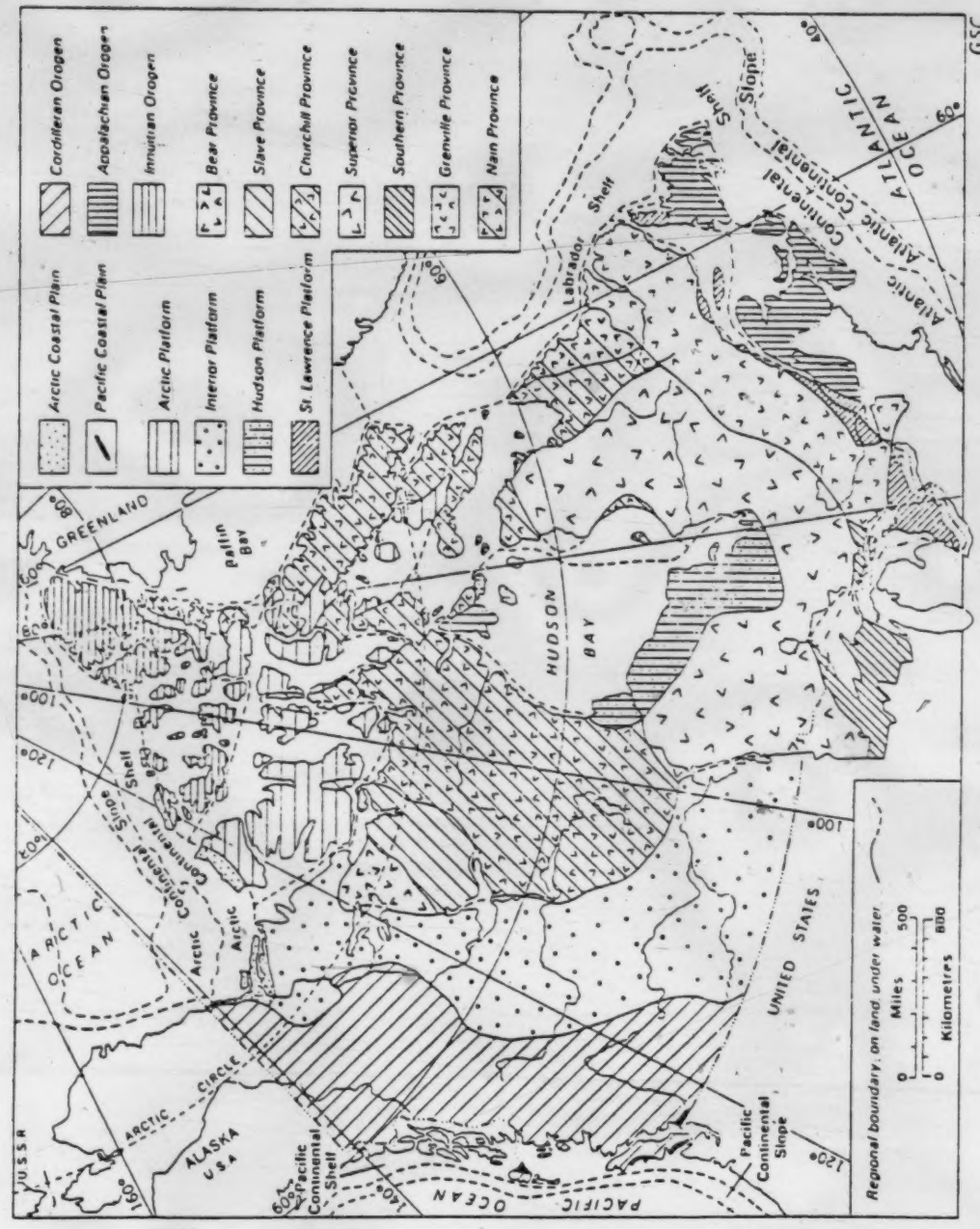


Figure 2.2 Map showing structural provinces in Canada (from Geology and Economic Minerals of Canada, 1970).

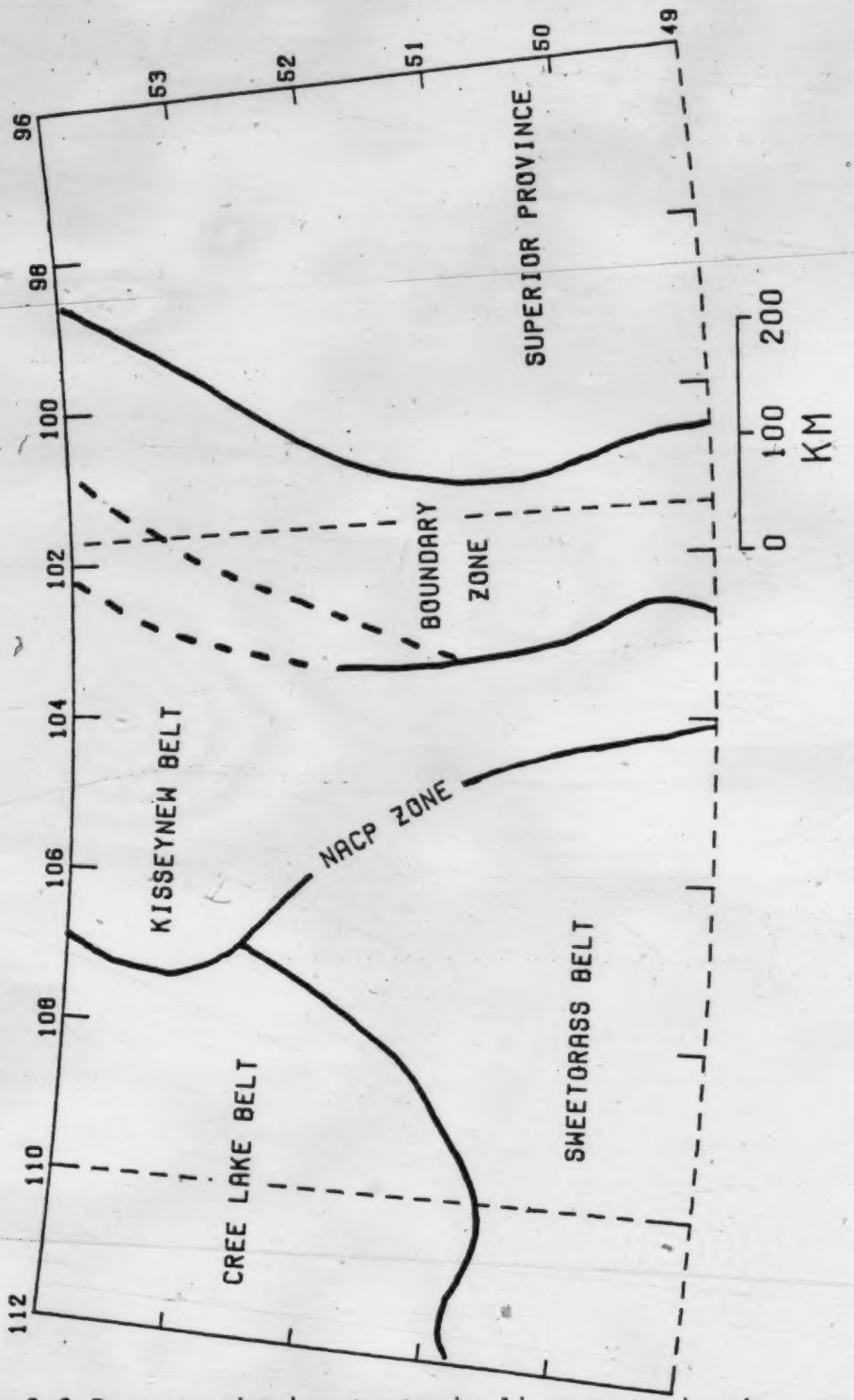


Figure 2.3 Basemap showing tectonic lineaments in the study area (modified from Sprenke, 1982).

The transition zone from the Churchill to the Superior province is known as the Nelson Front and is divided on the exposed shield into two subprovinces, the Waboden and the Pikwitonei belts. Granulite facies rocks of the Pikwitonei and amphibolite facies rocks of the Waboden belt both trend northeast-southwest. The Nelson Front is a geologic feature of tectonic significance. It extends at least 1600 km from Hudson Bay towards the international border. There is a great deal of controversy in the literature on both the width and location of the boundary zone. Width estimates vary from 1 km (Kornik and Maclaren, 1966) to over 200 km (Hajnal and Rose, 1979). Most of the proposed hypotheses are based on surface geology of the exposed shield and on qualitative analysis of potential field data.

The Wollaston fold belt in north Saskatchewan consists of interfingered pelitic schists, paragneisses and granites. This zone on the exposed shield has been correlated with a zone of very high conductivity known as the NACP anomaly (Camfield and Gough, 1977). This long narrow low resistivity zone is traceable across our profile at a longitude of about 105°W (figures-1.1 & 2.4). This anomaly was related to possible graphite schists associated with a fracture zone at the basement.

Another lineament of some tectonic significance lies to the west, between latitudes 50°N and 51°N (figure-2.3). This is a possible crustal rift discovered by Kanasewich et al (1969) which trends approximately east-west.

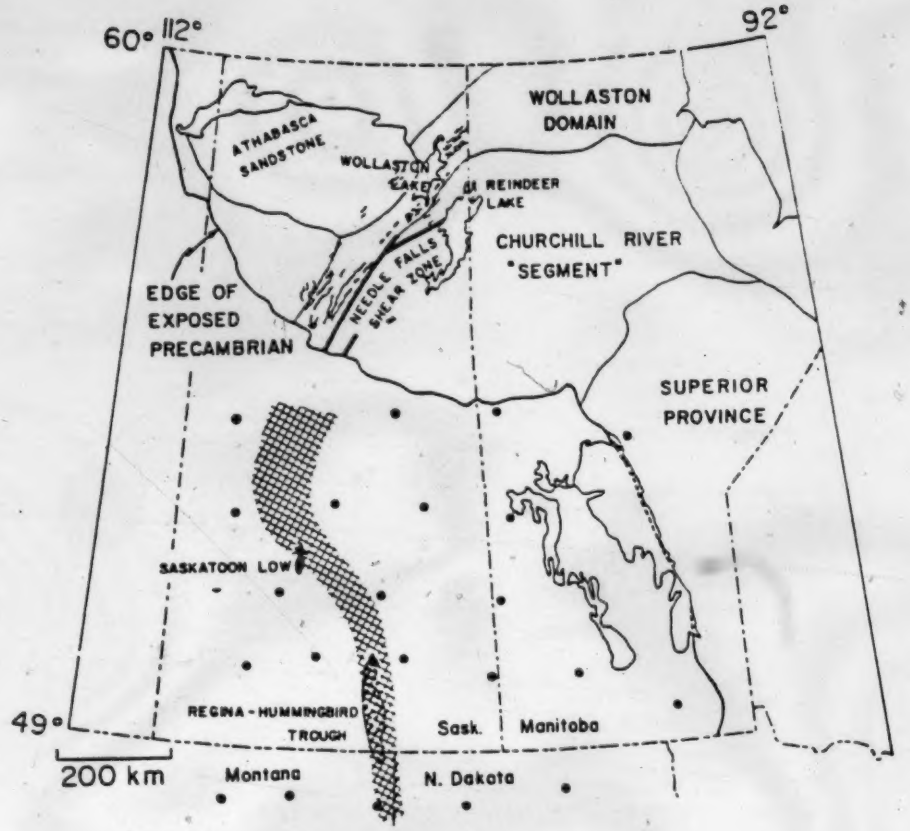


Figure 2.4 Geology of the northern part of NACP anomaly (after Camfield and Gough, 1977).

Further west, the Interior Platform is bordered by the Cordilleran orogen (figure-2.2) a geosyncline composed of Phanerozoic and Precambrian rocks which has been subject to deformations at various times. Folds and faults of the Rocky Mountains trend in a north to northwest direction.

**2.2 Gravity and Magnetic information:**

Figure-2.5 (gravity map) and figure-2.6 (magnetic map) indicate that our study area lies within a quiet zone of magnetic and gravity patterns. The sharp difference between western and central regions (at longitude 103°W) may represent a rapid change in lithology over a short distance probably indicating a north-south trending fault. Gravity and magnetic features of the Superior-Churchill boundary zone have been a matter of investigation since 1939. Recent studies (Green et al,1979) have shown that there are five distinct magnetic zones in the vicinity of our study area (figure-2.6). The important features are as follows:

(1) south central Saskatchewan is characterized by low magnetic relief similar to that exhibited by the Kisseynew belt of the Churchill province in the exposed shield.

(2) southeast Saskatchewan contains a zone of high amplitude narrow anomalies striking north. This zone is thought to be an extension of the Flin Flon belt beneath the sedimentary cover.

(3) along the Saskatchewan-Manitoba border, an area of low

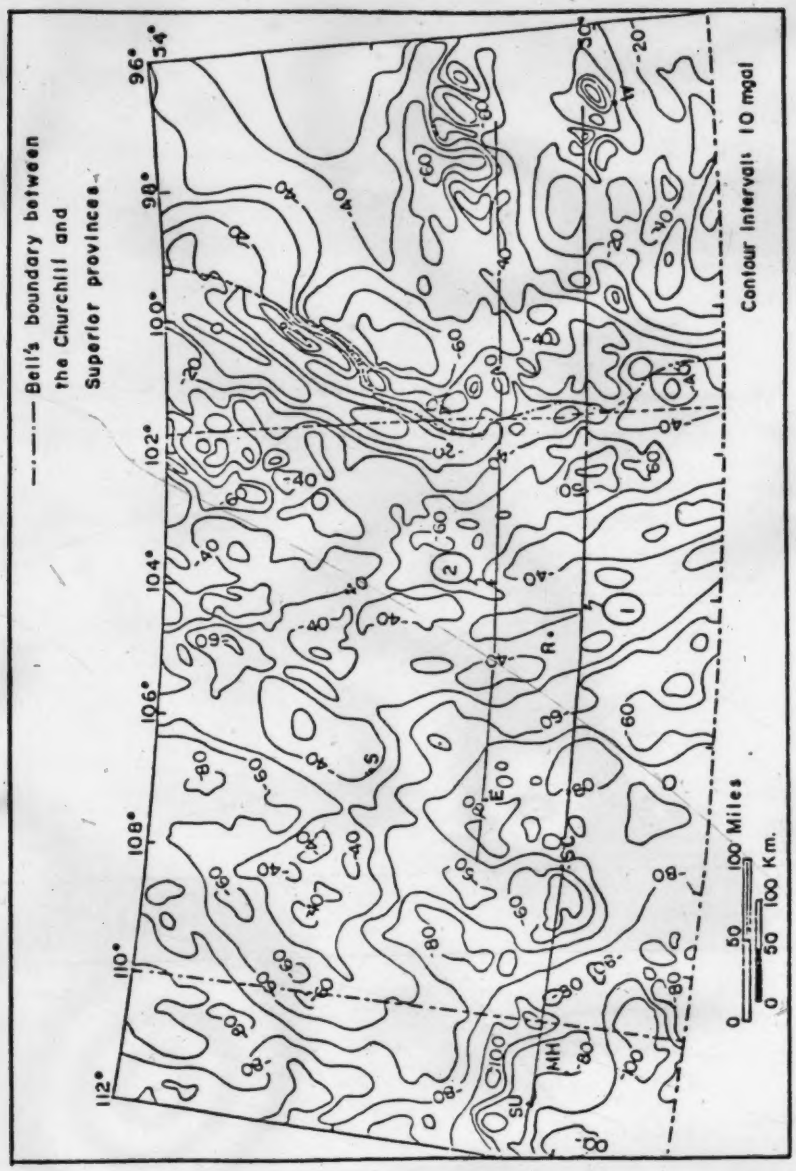


Figure 2.5 Bouguer gravity anomaly of southern plains (after Lee, 1977).

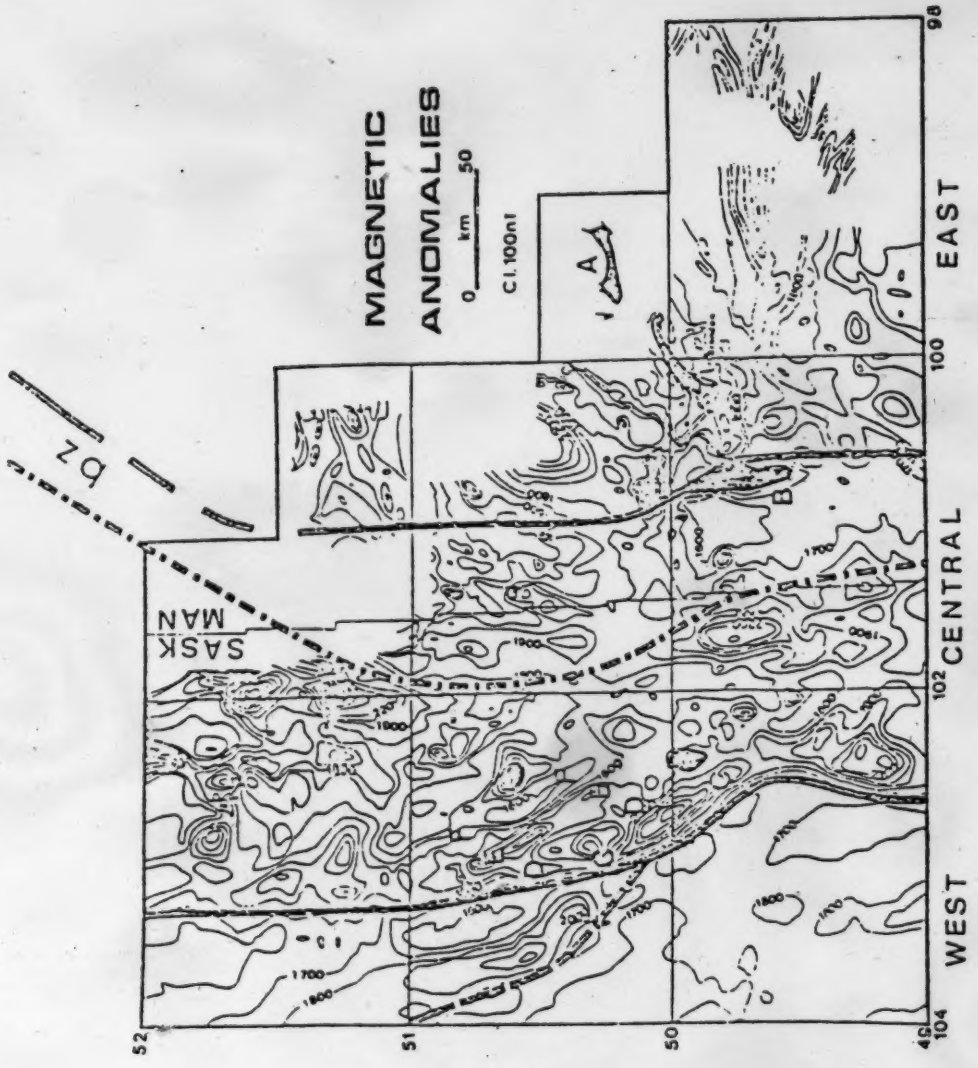


Figure 2.6 Magnetic anomaly map covering eastern part of the study area (after Green et al., 1977).

magnetic relief occurs, which is interpreted as the southern extension of the Churchill-Superior boundary zone.

(4) in south-western Manitoba, the magnetic anomalies show dominant east-west trends, an important characteristic of the Superior province.

The signature of the gravity pattern shows more or less similar trend directions and relief.

**2.3 Previous seismic studies:**

The central and southern part of the Interior Platform has been the location of a number of seismic refraction experiments (Steinhart and Meyer, 1961; Weaver, 1962; Maureau, 1964; Hall and Brisbin, 1965; Chandra and Cumming, 1972; Hall and Hajnal, 1973; Moon and del Landro, 1981) Interpreted results show an average crustal thickness of 47 km in southern Alberta and 39 km in northern Manitoba with upper mantle velocities between 8.1 to 8.4 km/sec. The studies also revealed the existence of a sub-basement layer of velocity 6.5 km/sec in the upper crust and an intermediate layer of velocity 7.1 km/sec (Riel discontinuity in Canada) in the lower crust. The Suffield-Swift Current profile (figure-2.7) which lies just at the western end of our profile will be an important reference for comparison.

In addition to the refraction studies, detailed reflection techniques have been used successfully in the

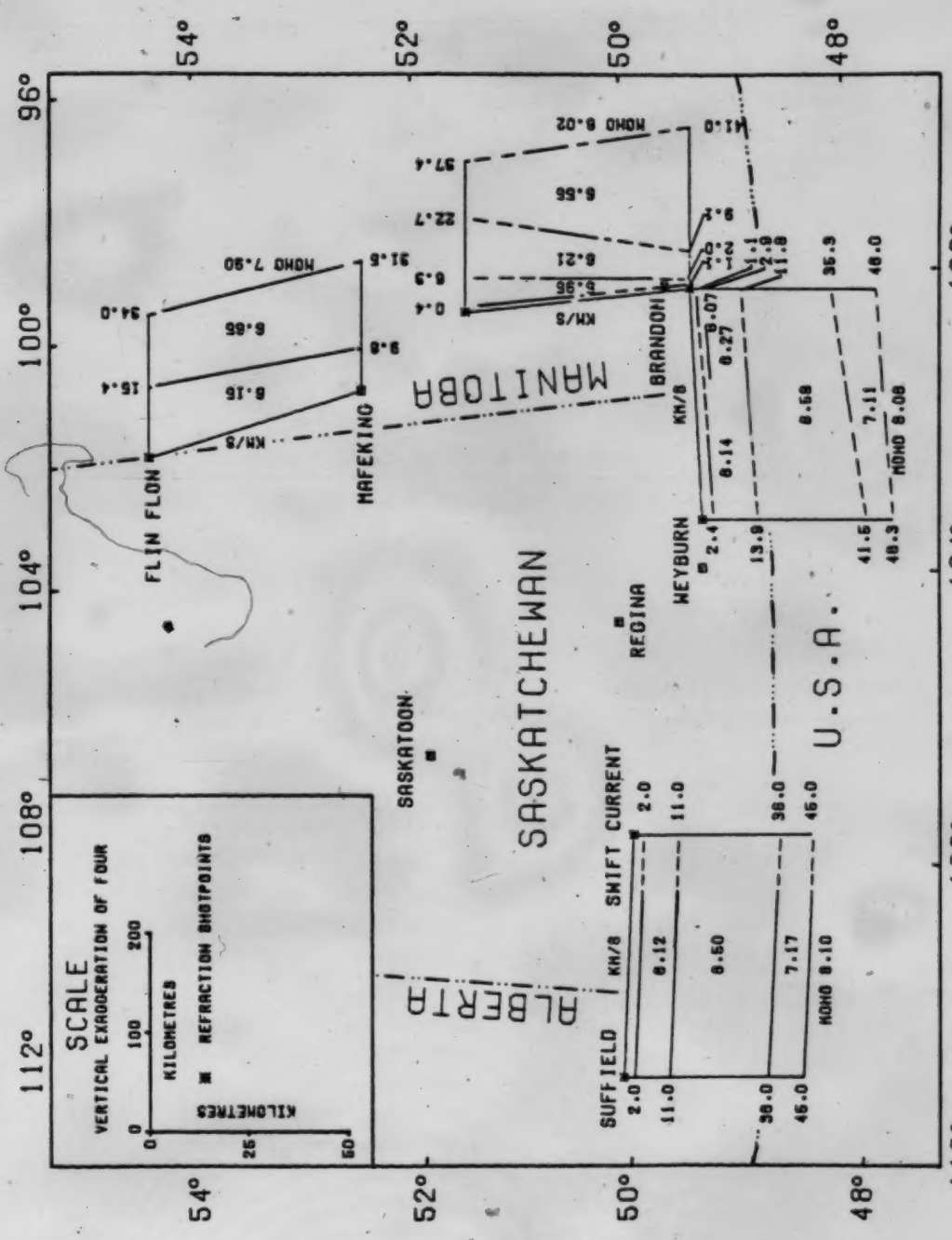


Figure 2.7 Crustal models from previous refraction experiments in Manitoba, southern Saskatchewan and southern Alberta (after Kazmierczak, 1980).

area (Cumming and Kanasewich, 1966; Clowes and Kanasewich, 1970; Sereda, 1978). The profiles show a complex earth structure including a number of dipping horizons within the crust with significant topographic relief. Combined refraction and reflection interpretations revealed the existence of a number of major faults in the middle and lower crust which in some cases penetrate the Moho discontinuity (Kazmierczak, 1980). The reconnaissance study of CO-CRUST 1977 and 1979 led to some general conclusions:

(1) the crust is thicker in the Churchill province than that in the Superior province. A major crustal fault might be responsible for this difference (Green et al,1979).

(2) the east-west profiles in southern Alberta, Saskatchewan and Manitoba show similar results for the upper crust.

(3) the Riel discontinuity is evident only in the Churchill province.

(4) the crust thins eastward.

Recently, combined modelling of seismic and gravity data has been carried out by Sprenke (1982). He noted that:

(1) the Superior province is characterized by a rather flat and featureless Moho surface to the north-east, but a strongly tilted surface in the south-west.

(2) the Nelson Front is coincident with a fundamental change in the nature of the Moho discontinuity.

(3) an area of thick crust in the extreme southeast may be related to the Williston basin tectonics.

(4) the NACP zone occupies a gradational zone between two

different crustal regions. In the east, crust is of uniform thickness while western part consists of a number of east-west trending blocks.

(5) the crust thins towards the east. An anomalous thinning of the upper crust occurs in the southern part of the Nelson Front.

## 3. DATA ACQUISITION & INSTRUMENTATION

The second cooperative seismic refraction survey of the CO-CRUST group in south-western Manitoba and southern Saskatchewan was carried out in 1979 and was designed to examine the structure of the crust in the Churchill province as a continuation of its previous studies about the nature of the Superior-Churchill boundary zone. There was some hope of finding out more about a possible major crustal fault running in a north-south direction to correlate with a prominent feature on the magnetic map (figure-2.6). The features which were of additional advantage for conducting a survey in southern Saskatchewan were as follows:

(1) easy access for shooting and recording due to a complete network of available roads.

(2) unconsolidated surface layer allowing easy drilling.

(3) a number of bore holes from oil companies supplying information about the overlying Phanerozoic sedimentary section.

(4) well defined gravity and magnetic expressions of the boundary.

The east-west profile which is the recording site of our data, extends from Limerick (latitude 49° 38.4" and longitude 106° 4.4") to Carlyle (latitude 49° 37.5" and longitude 102° 5.8") shown as line-C in figure-1.1. The University of Alberta team recorded the main blasts at Oungre, Laross, Melita and Roblin. The latitude and longitudes of the receivers were obtained from 1:50,000

topographic maps. A reading accuracy of 0.5 mm yielded the longitude and latitudes with an accuracy of 1.28" (about 25 meters). Two shots were detonated from Limerick to record the east-west profile. Charge sizes were 250 kg and 1375 kg respectively. Reciever numbers 18 to 33 recorded signals from the smaller charge while seismometers 1 to 17 recorded the larger shot. Time of shots, latitude, longitude and other shot parameters were compiled by Dr. Z. Hajnal of the Department of Geological Sciences of the University of Saskatchewan. Shot point to receiver distances were calculated using a geodetic computer program by supplying the geographical coordinates as input data. All refraction data were recorded on magnetic tapes. The recorder types used were EMR Digital and Analog FM recorders of the University of Western Ontario. Each system had its own characteristic gain and frequency response over a passband of 1-20 Hertz. Each receiver recorded at least 60 seconds of data samples after the first arrival. The elevation difference between seismometer positions were less than 100 meters. The recording sites did not deviate more than 4 kilometers from the linear profile on either side of it. The distance between shot point and farthest seismometer location was 287.2 kilometers and the receiver spacings ranged from 7 to 16 kilometers. All field data were redigitized at a rate of 60 Hertz for the digital instruments and between 58 to 61 Hertz for the fluctuating analog instruments. Data samples were put into a file of

1344 blocks, requiring a tape length of 58.61 feet (6250 BPI). Each record contained 7200 samples and the first three data words provided information about receiver number, shot number and orientation of the seismometers respectively. The data were written in format (5E16.6) with a block length of 1200 samples. Therefore each trace consisted of 24 blocks of data on the magnetic tape.

## 4. THEORETICAL CONSIDERATIONS

### 4.1 On the use of some basic parameters:

Applied stress from an explosion results in the propagation of the condition of the strain through the crustal medium as elastic waves. Depending on the direction of movements of the particles of the media there may be several kinds of elastic waves. In the case where the particles of the medium move in the same direction as the direction of the wave propagation, it is called the P-wave. There are three main P-wave groups usually observed in seismic crustal studies: Pg, PmP and Pn. These are described below.

*(1)Pg group:*

This group represents waves which penetrate into the upper part of the basement having a velocity between 5.5 and 6.5 km/sec. From field examples it has been found that the Pg wave may be complex in nature showing different subgroups from sedimentary rocks and the crystalline basement. In a continuous profile there may be several segments of travel time branches up to the point of intersection with the Pn branch and each segment is delayed with respect to the preceding one. The amplitude of the first phase becomes weaker with distance and the next delayed phase shows comparatively large amplitudes where it is first observed. At greater distances the later event becomes a first arrival

and the picture is repeated. This splitting feature may not be noticed if spacing of detectors is too large. The apparent velocity increases with distance and may even show a value between 6.5 to 7.0 km/sec. In such cases, these waves will have reached the middle or the lower crust.

*(2) PmP group (a reflection):*

This group bottoms at the crust mantle transition or boundary with an apparent velocity between 6.8 and 7.6 km/sec. If a more or less strong velocity gradient or a discontinuity exists between the crust and the mantle, a reversed travel time branch is generated. This wave appears as distinct secondaries and is characterized by larger amplitudes near the point of critical reflection. For a continuously observed profile a phase correlation for this group may be interrupted and split into separated segments. Instead of sharp onsets these reflections (or diving waves) sometimes may show a long duration sweep (0.4-1.0 sec) which indicates a broader transition zone. Splitting nature of the PmP may indicate a sandwich like structure of the crust (Fuchs, 1969; Clowes and Kanasewich, 1970; Giese, 1976). To join these separated segments in a single curve the principle of group correlation (see chapter-5) is applied. Apparent velocity obtained from the subcritical range is usually greater than that for supercritical range. Sometimes the velocity at supercritical range may show an apparent value equal to the maximum velocity of the Pg-waves.

*(3) Pn group:*

This wave penetrates the uppermost part of the mantle and has a velocity between 7.6 and 8.5 km/sec. This wave group is recorded as a first arrival at larger distances (beyond 130-220 kms). Recently the Pn wave has been interpreted as a refracted wave penetrating into a medium with weak positive velocity gradients rather than as a head wave. This branch disappears or is replaced by another delayed event after 300-400 kms. The amplitude recorded for this wave is often very small and is easily perturbed by local noise. The backward extrapolation of the Pn branch usually meets the PmP branch at the point of critical reflection. For the cases where Pn branch intersects the PmP branch it definitely means that the mantle wave Pn is associated with a greater depth than that of the reflected PmP and that there exists no plane interface common to both Pn and the PmP (Giese, 1976a).

**4.2 Apparent velocity:**

Near surface local inhomogeneities cause small scale irregularities in the travel time curves. For an average structure, we ignore the variations and compute the least squares velocities for different segments. This gives an average velocity estimation for the travel time branch under consideration. If however, we are interested in the velocities corresponding to each point of the travel time

curve, an interpolation method (Giese, 1976) can be used. Having three data points, the derivative dX/dT is determined by a second degree polynomial (Stewart, 1966):

$$dT/dX = \{(2X-(X_2+X_3))/(X_1-X_2)(X_1-X_3)\}T(X_1) \quad (1)$$
$$+\{(2X-(X_1+X_3))/(X_2-X_1)(X_2-X_3)\}T(X_2)$$
$$+\{(2X-(X_1+X_2))/(X_3-X_1)(X_3-X_2)\}T(X_3)$$

where, X is the distance at which the derivative is required. The velocity of interest is the reciprocal of the slope and T(X) is the travel time at offset distance X.

**4.3 Calculation of Depth:**

The exact determination of the velocity-depth function from the travel time data requires a number of preconditions. Therefore this task can only be solved by introducing some assumptions in order to overcome the lack of data. Consequently the solution is valid only within certain limits. It is useful therefore to have some simple methods which allow the determination of limiting values of parameters such as the possible maximum and minimum depths:

*(1) Maximum depth:*

From each point of the travel time curve, three quantities can be determined: (a) distance X (b) corresponding travel time T and (c) apparent velocity 1/Va = dT/dX. Assuming a homogeneous overburden structure of

constant thickness Z, a point from the reflection branch corresponds to a depth

$$Z = 0.5X\{Va.T/X - 1\}^{0.5} \quad (2)$$

For inhomogeneous media, however this value will give the maximum possible Z (Giese, 1976). The maximum possible overburden velocity can be estimated from

$$Vmax = \{Va.X/T\}^{0.5} \quad (3)$$

The maximum depth for progressive branches including head waves can be estimated from (Slichter, 1932; Berry, 1971):

$$Z = (1/n)X.\cosh^{-1}(Va.T/X) \quad (4)$$

*(2) Minimum depth:*

For a reversed branch with constant gradient structure the minimum depth can be obtained from (Giese, 1976)

$$Z = 0.5X\{(1-\sin\phi)/\cos\phi\} \quad (5)$$

where,

$\phi = \sin^{-1}\{V_0/Va(p)\}$

$V_0$ = velocity at the surface.

Va(p) = velocity at the maximum depth of penetration.

Depths for the points of a progressive branch is calculated

from ( Pavlenkova, 1968):

$$Z = 0.5X\{(Va.T/X-1)/(Va.T/X+1)\}^{0.5} \qquad (6)$$

where (X,T) are the coordinates of the crossover points between the refracted segments.

*(3) Depth from linear segments:*

For head waves, the first arrivals align in an approximate straight line segment. A least square estimate will give the best apparent velocity and intercept time from which the corresponding depths or thicknesses of the layers can be obtained. Thickness of the (n-1)th layer of velocity V(n-1) having an intercept time $T_0(n)$ is given by (Dobrin, 1976)

$$H(n-1) = 0.5T_0(n)V(n-1)V(n)\{V(n)^2-V(n-1)^2\} \qquad (7)$$
$$-\sum_{k=1}^{n}\{H(k)V(n-1)/V(k)\}\{(V(n)^2-V(k)^2)/(V(n)^2-V(n-1)^2)\}^{0.5}$$

This relation can easily be programmed in a computer to solve for thicknesses of multiple horizontal layers. Alternatively a simple stripping method can be applied. In this process a two layer formula (Dobrin, 1976)

$$H = 0.5T_0V(1)V(2)\{V(2)^2-V(1)^2\}^{-0.5} \qquad (8)$$

is sufficient to calculate thicknesses for n multiple layers. For the very first head wave branch this equation

essentially gives the thickness of the surface layer. Next, the first intercept on the time axis is used to reduce the receiver and the shot location at the base of the surface layer. Then using the same formula for the corresponding variables of the second head wave branch will give the thickness of the second layer. In this way we can proceed to determine thicknesses for multiple layers using the simple two layer formula.

**4.4 Exact solution:**

Herglotz (1907) and Bateman (1910) have independently given the solution to the problem of inverting travel times into velocity depth values. Wiechert (1910) simplified the formula and thus the application becomes easier. Independently from the final form of the theorem the following conditions must be met:

(1) the function T(X) must be continuous between X=0 and X=Xp that is, an interruption is forbidden.

(2) the apparent velocity along the curve, starting from X=0 must increase monotonically.

(3) the derivative dX/dT must be continuous along the travel time curve.

There are several different forms to present the solution of the integral equation:

$$Z(Vp) = (1/\pi)\int_{o}^{X_p} \cosh^{-1}\{Vp/V(X)\}dX \qquad (9)$$

where,

Vp = velocity at maximum depth of penetration.

Xp = corresponding offset distance.

V(X) = velocity at arbitrary distance X.

For low velocity zones an alternate extended form of this equation can be used (Gerver and Markushevich, 1967).

There are several ways to approach the integration of the WHB equation for practical purposes. The simplest way is to fit the travel time branch to a polynomial

$$T(X) = C_0+C_1X+C_2X^2+C_3X^3+.... \qquad (10)$$

The order of the polynomial is chosen from the condition of best fit. The approximate function T(X) is now differentiable in any domain of X. Thus the quantities Vp and V(X) are easily obtained by simple differentiation of T(X) at distances Xp and X. The integration may be performed by simple methods such as the Simpson or Trapezoidal rule.

**4.5 $T^2$-$X^2$ method:**

This method is based on the assumption of straight ray paths in the overburden and the existence of a first-order discontinuity as a reflecting horizon. For the subcritical portion of the reflection branch both conditions are met to a good approximation. A plot of $T^2$ versus $X^2$ gives a

straight line with an intercept $(2Z/V)^2$ whereas the slope is equal to $1/V^2$. V specifies the average overburden velocity above the discontinuity.

When applying $T^2-X^2$ method in crustal studies one has to confine oneself to rays refracted as little as possible but which are clearly observed in the records. If all the discontinuities are represented in the travel time curves, these branches can be used to estimate interval velocities according to the Dix formula (Dix, 1955):

$$Vi = \{(V_2^2T_{2o}-V_1^2T_{1o})/(T_{2o}-T_{1o})\}^{0.5} \qquad (11)$$

where,

Vi = interval velocity.

$V_1$, $V_2$ = velocities from the first and second branches respectively.

$T_{1o}$, $T_{2o}$ = intercept times for the first and second branches respectively.

Estimations of interval velocities are useful in that they can reveal information about velocity decrease or low velocity zones within the interval considered, which are not readily obtainable from refraction data alone.

**4.6 Theoretical seismograms:**

Interpretation of seismic data based on travel times or apparent velocities alone are not enough. For a complete analysis of the data both kinematic and dynamic properties of the wavelet must be examined. Synthetic seismograms can be used as an aid to the body wave interpretation. Several methods have been used recently to compute theoretical seismograms for seismic modelling. Examples of the main techniques are the reflectivity method (Fuchs and Muller, 1971), the generalized ray method (Wiggins and Helmberger, 1974), Disc ray theory (Wiggins and Madrid, 1974; Wiggins, 1976), Full wave theory (Cormier and Richards, 1977) and the WKBJ seismogram (Chapman, 1978; Dey-Sarkar and Chapman, 1978). Among these several techniques some are computationally very expensive and their use is limited to a few trial models. We have chosen the Chapman WKBJ seismogram because it is cheaper to calculate and is effective for limited bandwidth body wave interpretation. The solution of a point explosion in a spherically symmetric and isotropic medium is obtained by taking the Fourier transform with respect to time, of the equations of motion and the constitutive equations and expanding the displacement and stress parameters in spherical harmonics. A ray expansion method is used to solve the radial ordinary differential equation with boundary conditions at the free surface, at the center of the sphere and at interfaces appropriate to the ray of interest. Then this

ray-transformed response is converted to the response at the receiver position by evaluating its inverse Fourier transform. Only outward travelling waves are considered with a far field approximation which requires that the property of the media should change little within one seismic wave length.

Practical limitations of seismic interpretations using synthetic seismograms are a result of limitations of the computational method and the complexities of the observed records. For many regions within the earth, the assumptions of the simpler theoretical models, particularly of lateral homogeneity and no attenuation, are poor approximations. Comparison of synthetic with observed records requires a knowledge of the source waveform. Moreover, observed seismograms require amplitude corrections which may be inaccurate because of inadequate knowledge of the instrument response and especially the near surface site response.

Although several difficulties in interpreting seismograms remain including insufficient data, ambiguity of interpretation and inadequate mathematical treatment, significant insight to interpretation can be gained through analysis of synthetic seismograms and comparison with the observed field records.

**4.7 Low velocity zones:**

Gutenberg (1955) suggested the existence of low velocity layers in the crust. This idea was again picked up in the beginning of the sixties when detailed data from explosion studies became available. Landisman et al (1971) have given a detailed discussion of the existence of low velocity zones in the upper and middle crust. There are two possibilities of detecting a velocity inversion within the profile under study:

(1) having a series of wide angle branches in the seismogram, average overburden velocities can be calculated using $T^2-X^2$ method. Calculation of interval velocities from overburden velocities may reveal information about a low velocity layer in the crust.

(2) according to Snell's law a low velocity causes an interruption of the travel time curve. A jump in the time and distance is generated between two branches which is spent in passing through the low velocity region.

By careful study of the observed seismogram other indirect evidence for low velocity zones may become clear. Among these secondary diagnostic features are the strong late arrivals after several tens of kilometers (Landisman et al ,1971), rapid attenuation of pure head waves with distance and absence of associated head waves corresponding to a particular reflection branch.

Demonstration of the existence of a low velocity zone requires travel times from high quality refraction profiles

in combination with reflection times and amplitude data. The sialic low velocity zone possibly caused by intrusions has been proposed by Landisman et al (1971) to have a lower boundary at depths of 10-15 km. Another velocity inversion in the middle crust was proposed at 20-28 km depth which could be associated with a region of high conductivity in the crust (Landisman et al, 1971). Owing to the existence of low velocity zones the task of inverting T(X) data into the V(Z) domain leads to a nonunique solution. However once the time and distance spent in the low velocity layer is determined the corresponding portion of the travel time branch can be subtracted from the total time and distances to re-establish the continuity of the travel time curve as demanded by the WHB method. Slichter (1932) and Gerver & Markushevich (1966) have given solutions to the low velocity problem. Recently synthetic modelling has been found suitable for detecting low velocity layers in the crust (Braile and Smith, 1975) when reliable amplitude information exists. In chapter-6 we will use $T^2$-$X^2$ analysis and synthetic modelling technique to establish the presence of low velocity zones under the study area.

# 5. DIGITAL PROCESSING

## 5.1 Presentation of seismic records:

The simplest method of data presentation is to plot the full seismic record using shot instant and location as the zero reference. Such presentation requires a large page size, or a very small scale however, and it is much more useful to have a large scale plot retaining all the necessary information in it. Therefore a reduced travel time plot was used for overall display and processing purposes. A reduced time T' is defined as

$$T' = T - X/Vr \qquad (12)$$

where,

X = offset distance.

Vr = reduction velocity.

Vr was chosen to be equal to 6.5 km/sec for most of the data in this thesis. The significance of Vr is that if this velocity is close to the apparent velocity of the waves of interest it will produce a display showing the phases of 6.5 km/sec velocity arranged in a horizontal line. This kind of display facilitates the correlation process (see section-5.4). If the velocity of interest can not be specified an average velocity of the crust is used as the reduction velocity.

The channel separation should be as short as possible ensuring clear readability. Uniform spacing of the traces was not possible due to variable seismometer distribution.

No elevation correction was applied for two reasons:
(1) such correction would require the knowledge of near surface velocities in detail.
(2) the amount of correction would be small since the difference between station elevations was small (less than 100 meters).

Since we planned to process only the P-wave phases, all record sections show only the traces for vertical component seismometers. The average spacing between receiver stations were about 12 km. A time scale of 0.5 inch/sec was used to accomodate the plot within the page size. A time correction was applied to display each record from the zero reference time, which we selected to be the shot point time.

In the complete record section, amplitude information is a very desirable characteristic to retain but in practice it seems to be very difficult due to the following reasons:
(1) quantitative determination of the amplitude-charge relation is very difficult to attempt.
(2) frequency characteristics of individual seismometers are different.
(3) seismometer coupling may be variable.
Two different methods were tried for normalization:
(1) correct response of the seismometers were restored by dividing each trace by its gain factor. Since at large

distances the head wave amplitude varies as $1/X^2$ all traces had to be multiplied by an inverse of this factor. Then a common dividing factor was estimated to bring the maximum amplitude of the nearest (to shot) record to unity.
(2) each trace had maximum amplitude equal to unity.
In both cases the mean value of each trace was removed from the trace before normalization.

It was evident that even with a variable seismometer response, method-1 was more helpful for correlating the secondary events. At least it gave some idea about the relative amplitudes of the signals. However, a number of records required amplifications before approximate relative amplitudes could be ensured. This is presumably due to variations in seismometer coupling, although other causes are possible and are discussed later.

**5.2 Spectral analysis:**

As a consequence of the general availability of large computers the technique of spectral analysis of seismic data has come into much use during the last few decades. The usual seismic record displays the amplitude as a function of time (in the time domain) whereas a spectrum shows amplitude as a function of frequency (in the frequency domain). The phase of a seismic wave can also be displayed as a spectrum which is known as the phase spectrum. Evaluation of spectra yields very important information about the source and the

medium traversed by the signals.

The application of the Fourier transform converts the time domain information to that in the frequency domain. For lengthy data usually a moving window is used to estimate the spectra at consecutive window positions. Since truncation of data by a window creates side-lobe effects the window in the frequency domain is chosen to be as smooth as possible.

Raw spectral estimation was carried out for a series of records with increasing distance (figures-5.1 & 5.2). The length of each record taken for spectral estimation was of the order of 8 seconds after the first arrivals. Most of the useful seismic information was within this interval. Maximum signal energy was found to be restricted to a frequency band of 3-15 Hertz. The main peak of the spectrum was observed between 3.5-6.0 Hertz. A progressive lowering of frequency with distance is evident. A lower frequency of the main band compared to that of the usually observed signals may be explained as due to the shot hole environment. A small change in the frequency content of the main peak with distance may reflect a near homogeneous structure along the travelling path. There is a spectral peak at 10-12 Hertz corresponding to a distance of 58 km from the shot point. This peak gradually dies out at 104 km. Smaller peaks visible in the spectra can be considered due to signals generated within the crust by scattering or other secondary effects.

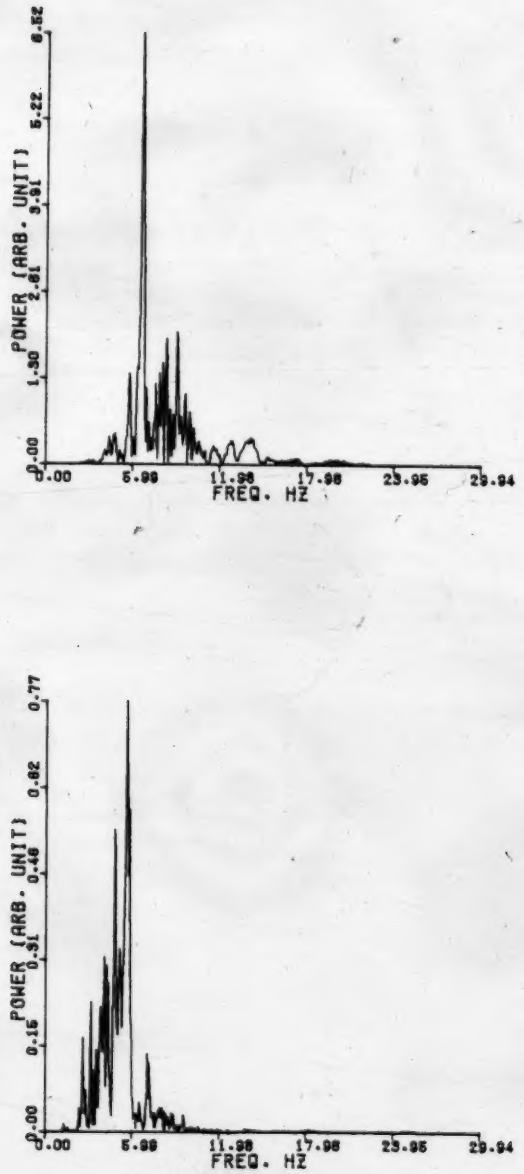


Figure 5.1 Power spectrum for records at distances 12 and 31.5 km from the shot.

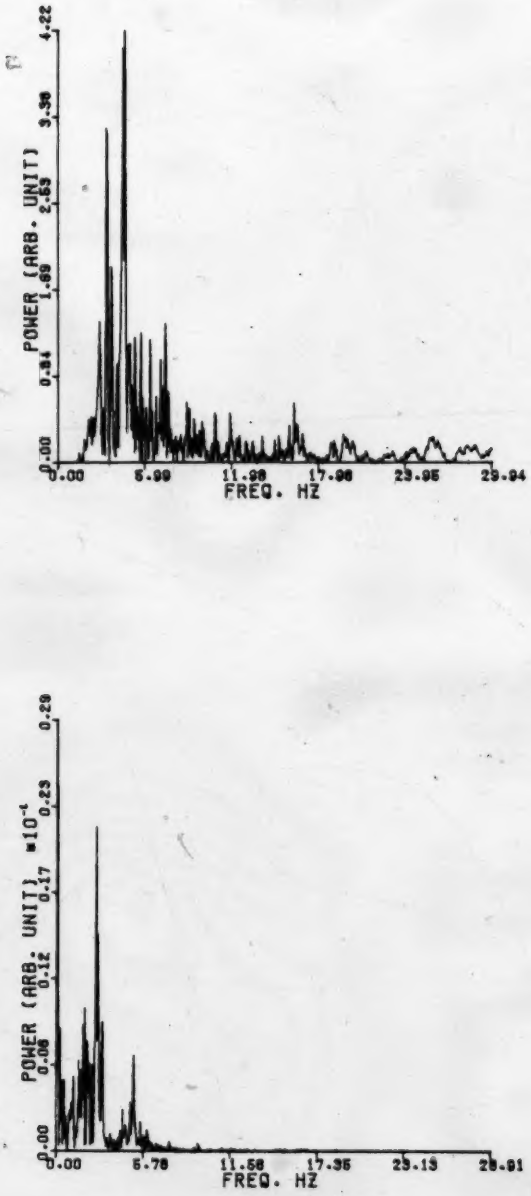


Figure 5.2 Power spectrum for records at distances 59 and 95 km from the shot.

**5.3 Digital filtering:**

Filtering means separation, that is, we separate out the part of the record we want to study and eliminate other simultaneous but unwanted parts. In order that filtering should be successful it is necessary that the wanted and unwanted wave motions differ in some property. To improve the signal to noise ratio in the seismogram, differences in the following properties can be used: frequency spectra, apparent velocity, wave polarization and spatial correlation. Frequency filtering is a relatively common and simpler technique used in the field of refraction seismology. Although the noise and signal spectra overlap over a wide band of frequencies, we selected the frequency filtering because of its simplicity and reasonable effectiveness. Zero phase shift eight pole recursive Butterworth & Bessel filters were used for bandpass filtering (figure-5.3). A discussion about the comparative effectiveness of these filters can be found in Chiu (1982). It was shown that:

(1) the Bessel filter has very little distortion and time shift effect on the first breaks but does not suppress noise as efficiently as the Butterworth filter with the same general characteristics.

(2) the Butterworth filter can suppress the unwanted parts more efficiently than other similar filters due to the rapid falloff in response outside the acceptance band but it distorts the first arrivals significantly.

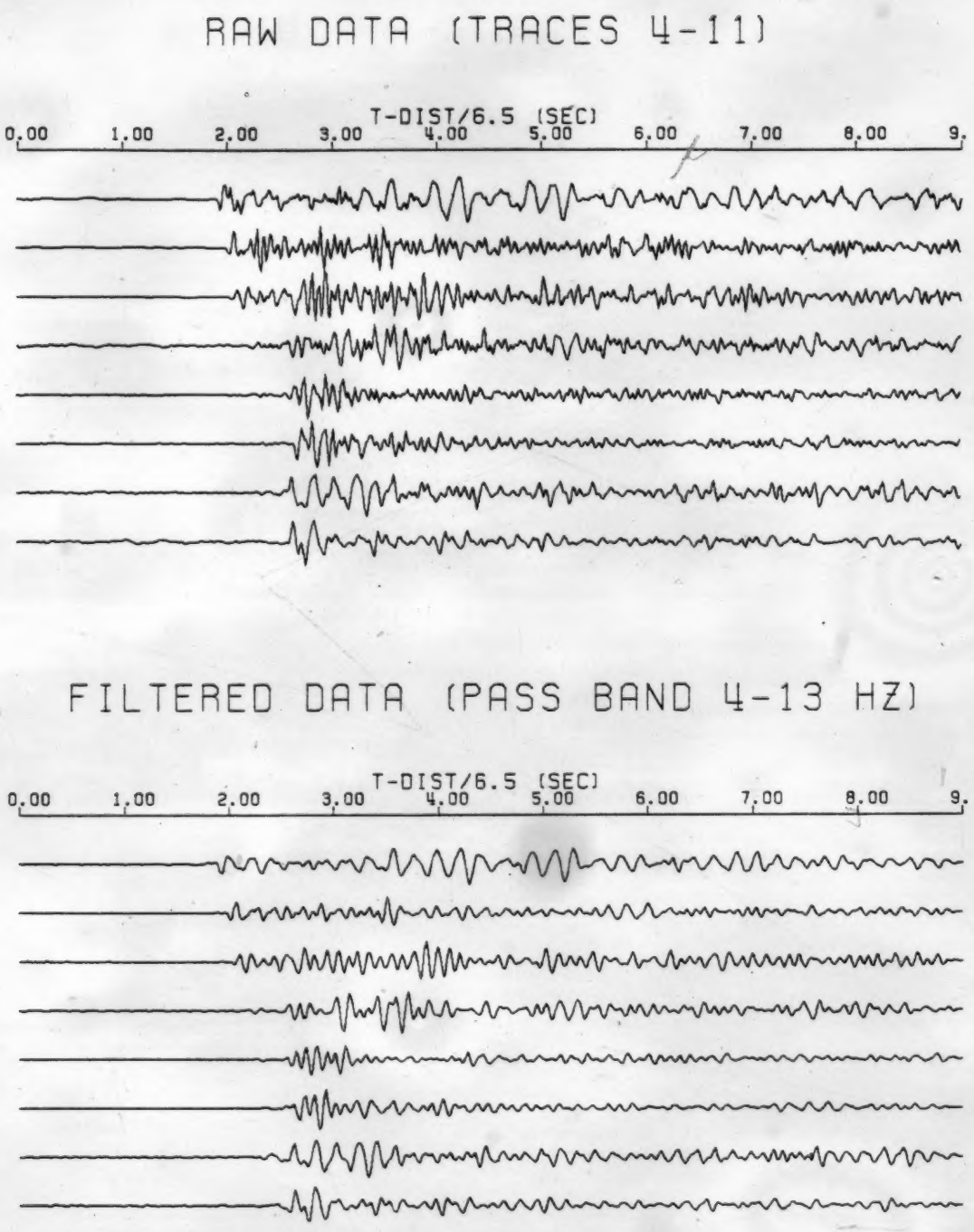


Figure 5.3 Example showing frequency filtering using an eight pole Butterworth filter.

We therefore used the Bessel and Butterworth filters respectively to study the first arrivals and the secondary events in the seismogram. The purpose of the filtering process was two fold:

(1) to get rid of the ground noise without affecting the first breaks and thus get a seismogram for overall display purpose (figure-5.4)

(2) to enhance the secondary arrivals (figure-5.5).

For the first case a Bessel filter with a band width between 4 to 15 Hertz was found suitable. For the second case a 6-13 Hertz Butterworth filter was used. The later process improved the secondary arrivals significantly and aided in correlating the later events.

**5.4 Correlation:**

Correlation implies fitting curves or straight lines to the same event on different traces. When correlating, the seismologist looks for three important properties: (1) character (2) amplitude and (3) frequency of the waves. Phase correlation is difficult if recording spreads are not continuous. Geophone spacings of less than 1 km is reasonable for this purpose. But if however this condition is not met, one has to rely on group correlation techniques, although velocity estimation from this method may differ from that of the phase correlation (Giese, 1976). Correlation of the first breaks are facilitated if the

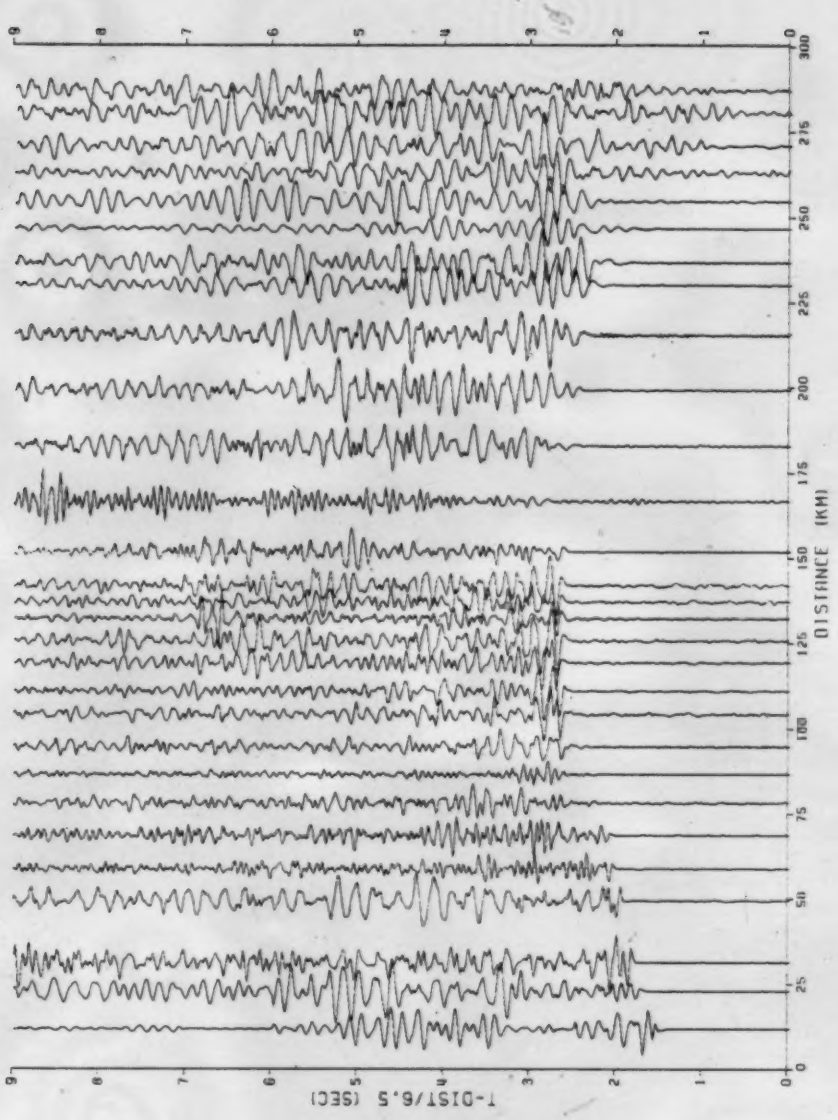


Figure 5.4 Vertical component seismogram of line-C from CO-CRUST 1979 refraction experiment (Filter 4-15 Hz Bessel).

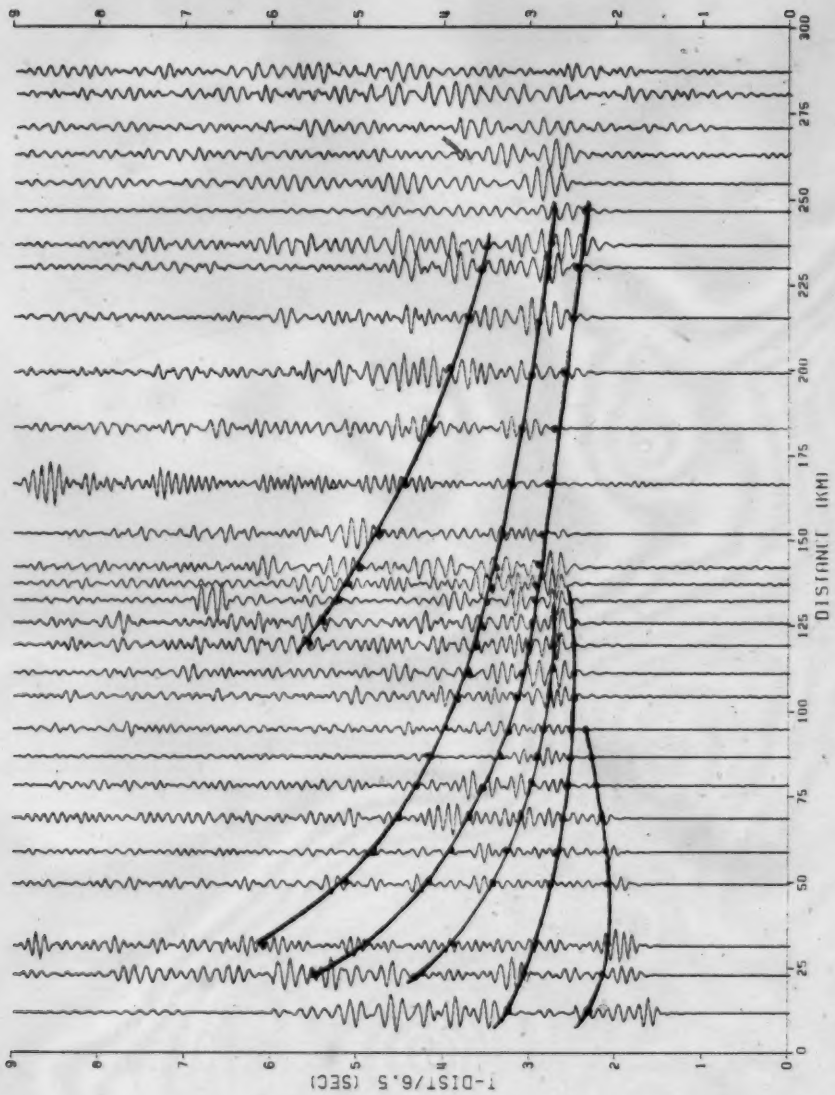


Figure 5.5 Seismogram of line-C showing correlated reflection events from CO-CRUST 1979 refraction data (Filter 6-13 Hertz Butterworth).

reduction velocity is close to the velocity of interest. The choice of channel separation is a compromise between clear readability and smallest possible detector spacing. Usually the first peaks or troughs after the beginning of a particular event are correlated. Then a small correction of the order of 0.10 sec is applied before calculating depths. This correction is also applicable to the intercept times. The main criteria for the correlation process are as follows:

(1) amplitude of events being correlated must exceed those of the noise.

(2) travel time branches must be of some length if they are to be identified with certainty.

(3) the apparent velocity must show values within a possible and reasonable range.

One has to be very careful when correlating events, because once the correlation has been made many aspects of the final model are fixed. This is especially true for a single profile interpreted in terms of a plane horizontally layered model, since correlation here exactly defines the velocities and ultimately the layer thicknesses, except in cases of ambiguity of low velocity zones. Amplitude information is also important. If relative amplitudes are not reflected exactly, one might correlate wrong events together. Attenuation causes progressive lowering of frequencies. Therefore when correlating, it should be remembered that the wave shape might change with distance as

well. The fact that we have used two different shots for recording a single profile might cause amplitude differences due to the variation in the charge sizes.

## 6. RESULTS AND INTERPRETATION

The interpretation of the refraction data from the east-west profile includes the analysis of results obtained from the horizontal layer model, WHB inversion, $T^2$-$X^2$ method applied to possible reflected phases and finally the synthetic modelling. The final model is a combination of all the separate models which best fits the observations. Although it is not possible to explain all the features of the observed seismograms, an attempt was made to accomodate the maximum possible numbers of important features in the final model.

### 6.1 Horizontal layer model:

The direct arrival can be identified only on the first record at 11.755 km from the shot point. Due to the large spacing between shot point and the first seismometer location, we probably missed detail and convincing information about the direct wave. From the slope of the line joining the only direct phase to the origin of the plot, we estimated the sedimentary velocity to be 3.64 km/sec. We compared this value to the available well data obtained from nearby locations. The formations above the basement indicated an average velocity of 3.2 km/sec for the sedimentary layer. The difference is small but we preferred the value 3.2 km/sec for further analysis because velocity estimation from a two point segment is rather unreliable.

The next arrival is more well defined. Events were recorded clearly up to 70 km and permit an exact phase correlation. The velocity picked up from the arrivals up to 35 km yield an average value of 5.97 km/sec. The rest of the arrivals indicate a slightly increased velocity, the least square estimate of which is 6.2 km/sec. It is possible that these two sets of arrivals correspond to a single basement layer with a positive velocity gradient in the lower part, but definite conclusion about this was not possible due to sparse receiver locations. The first arrivals after 70 km are very weak and delayed by about 0.1 second. Careful study of these arrivals were very important because of the following reasons:

(1) ambiguity of interpreting these arrivals as a continuation of the 6.2 km/sec phase due to the observed delay.

(2) the weak phases could also be interpreted as a part of the reflection branch from a possible interface at 11 km depth.

(3) since the NACP anomaly crosses our profile at about 105°W longitude, a study of the signal amplitudes between 50 and 100 kms from the shot point was particularly important to verify the possible effects of the conduction zone on these arrivals.

We therefore took special precautions to read the exact amplitudes within 100 kilometers from the shot. Three different normalizing methods were tried:

(1) each trace was divided by its gain factor to restore the exact response. The effect of $1/X^2$ attenuation of the head waves at large distances was minimized by multiplying each trace by $X^2$. Each trace was then normalized with respect to the average ground noise amplitude observed before the first arrivals (figure-6.1).

(2) this method was similar to the first one except that the traces were normalized with respect to the average noise level obtained from the far end section of the traces, on the assumption that shot generated noise should be of equal amplitude on each trace.

(3) this method tried to minimize the variable seismometer responses between 70-100 km from the shot point. Amplitudes of the refracted/reflected arrivals from the next layer were adjusted to a constant value to observe the resultant variations on the first arrival signals of interest (figure-6.2).

Detailed study of the amplitudes revealed that the weak pulses are reversed in phase with respect to the 6.2 km/sec arrivals and can be interpreted as reflection arrivals from an interface at 11 km (obtained from $T^2$-$X^2$ method discussed in section-6.3). According to Braile and Smith (1975) this however indicates a low velocity layer in the lower basement (figure-6.2 & 6.3). Therefore the horizontal layer interpretation was no longer valid for this region. We therefore used the $T^2$-$X^2$ analysis and synthetic modelling technique to justify this low velocity in sections 6.3 and

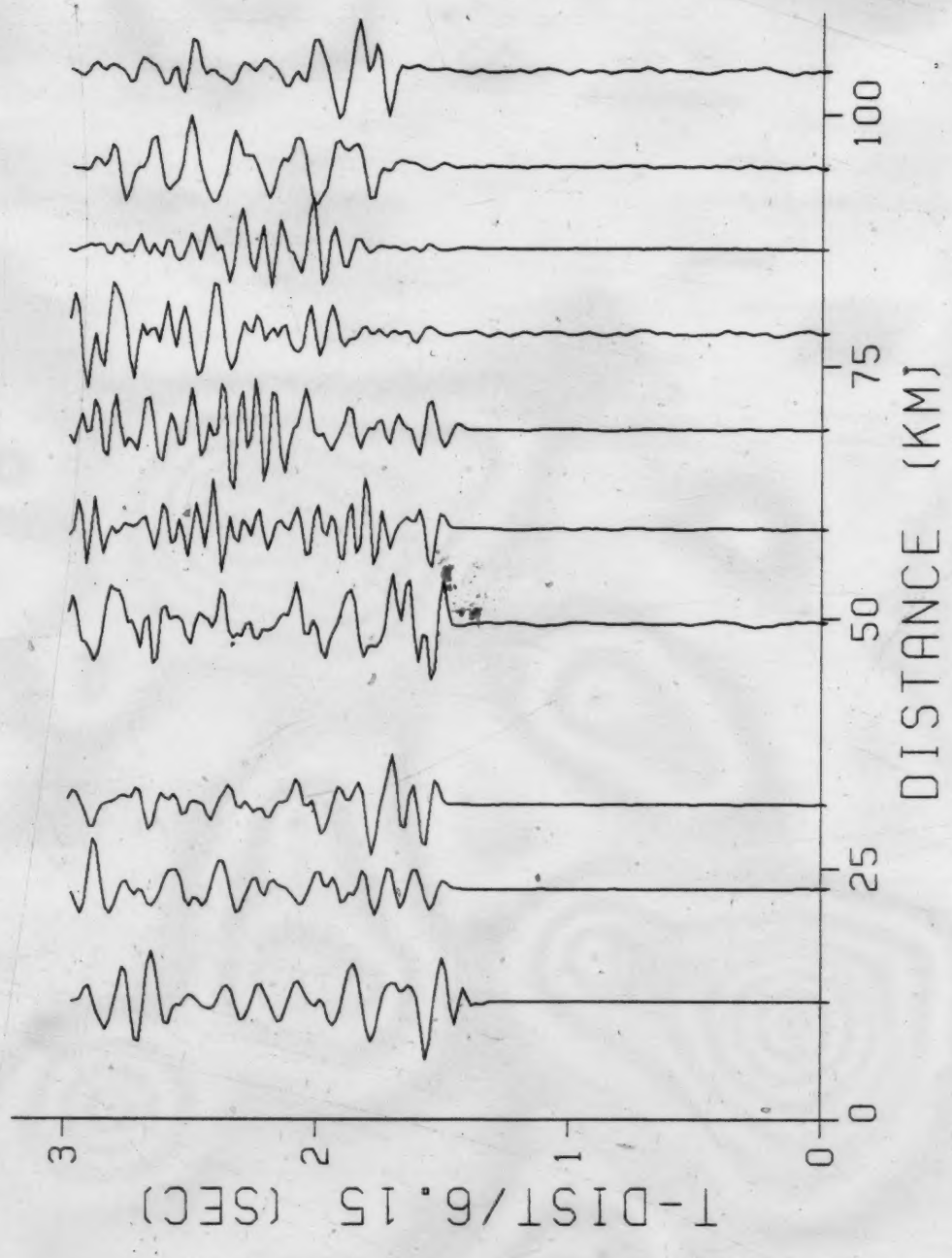


Figure 6.1 Normalization of traces with respect to the average noise level before the first arrivals.

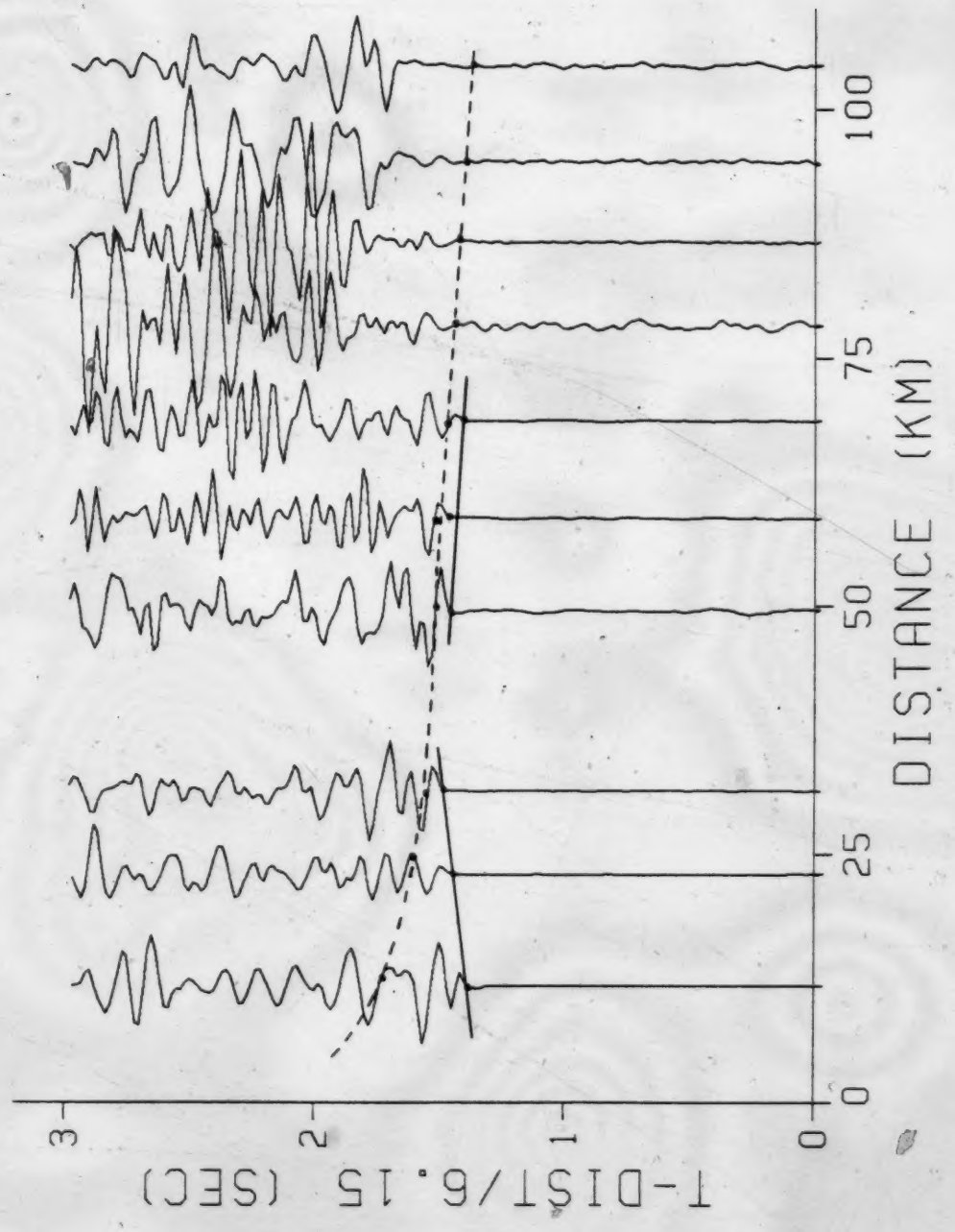


Figure 6.2 Normalization of traces keeping amplitudes of the prominent phases constant.

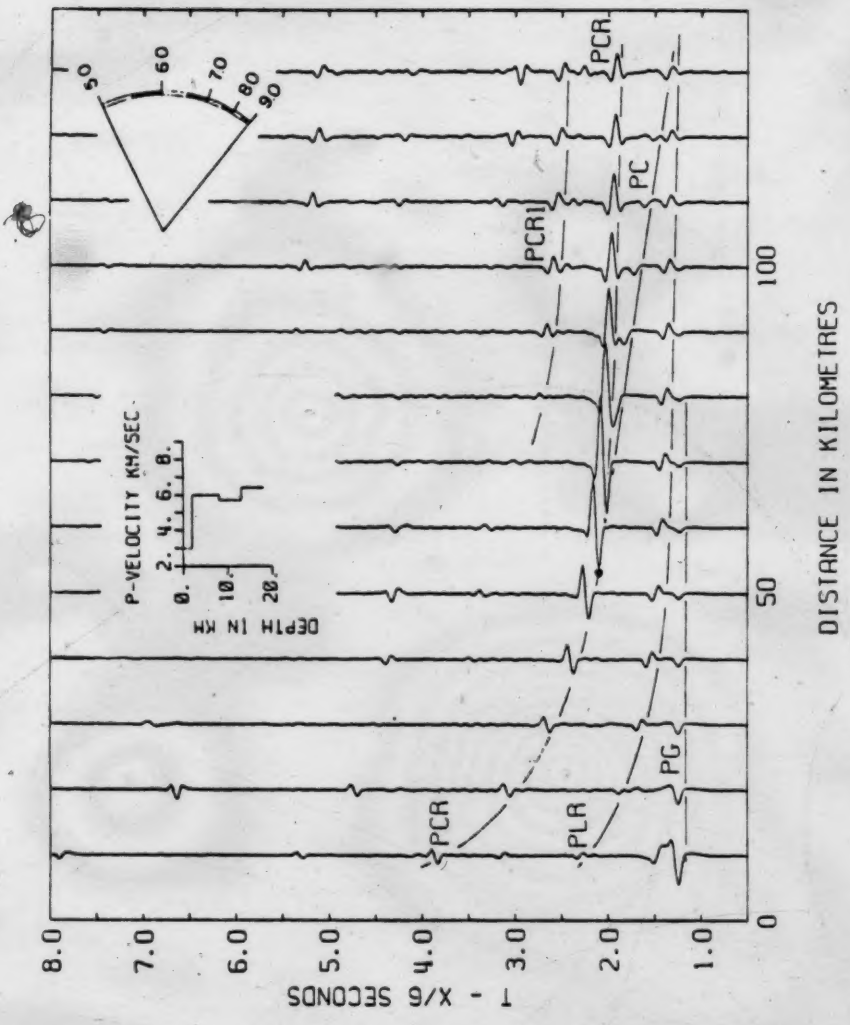


Figure 6.3 Synthetic showing arrivals (PLR) from top of the low velocity layer in the basement. PC, PCR & PCR1 specify the refracted, reflected and multiple reflected branches from the sub-basement layer (after Braile & Smith, 1975)..

6.4. The depth of the basement computed from the average velocity of 6.1 km/sec layer and the observed intercept time (using equation-7, chapter-4) corresponds to 3.03 km. The uniqueness of this value can be justified from the well log information as well. We computed theoretical intercept times from the total time spent in each layer and compared it to the observed intercept time in the seismogram. The two values were 1.45 and 1.34 seconds as determined from well log data, and as observed on the seismic profile. If we allow a correlation error of 0.11 second (which also includes the effect of a possible gradient zone), this implies a fairly good agreement. We list the computed parameters from well logs and the observed data in table-6.1. Most of the well logs were situated northward, a few tens of kilometers away from the profile. Since the Williston basin gets shallower to the north, a shallower basement to the north of our profile was confirmed by the well data. The increased depth of the basement as observed southward by seismic studies therefore does not contradict the well data obtained from the north.

A secondary phase corresponding to an apparent velocity of 4.1 km/sec was identified in the observed seismogram. (figure-6.4). Since this phase is absent in the radial component seismogram, it could be interpreted as a P-wave arrival from the lower sedimentary section. The computed thickness and depth of this layer are 2.0 and 1.5 kms respectively. Since we lacked further evidence to confirm

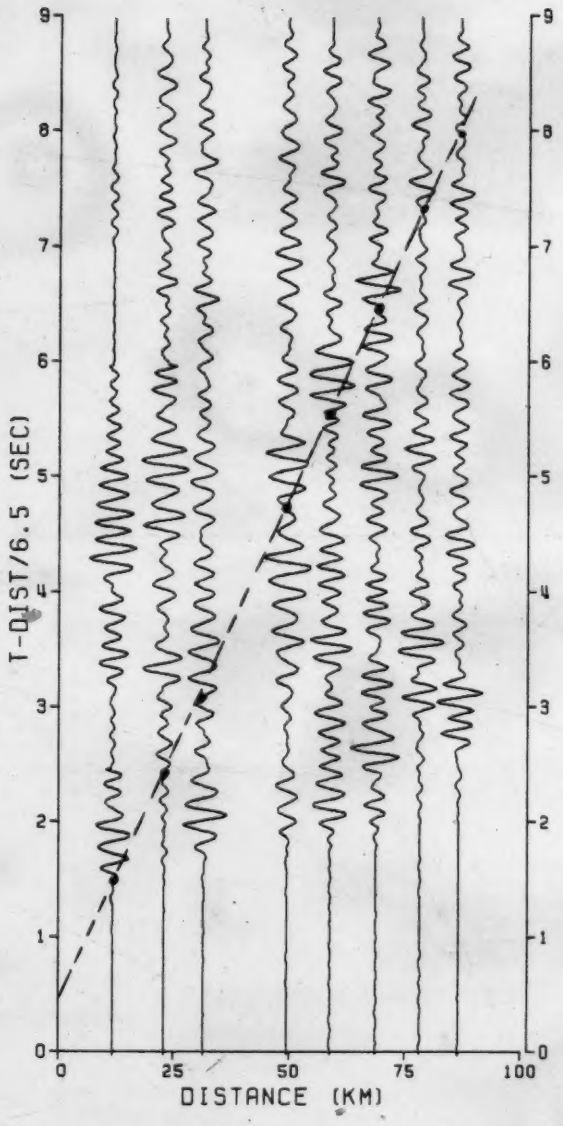


Figure 6.4 Correlated secondary arrivals corresponding to a possible layer of velocity 4.1 km/sec (filter 3.5-8.5 Hertz Butterworth).

this layer we ignored this secondary event while calculating the final model.

The next set of aligned phases are very prominent from 70 km to 140 km. The apparent refractor velocity from least square analysis is 6.49 km/sec. These arrivals are followed by another onset having an apparent velocity of 6.7 km/sec which appear as first arrivals between 150 and 230 km from the shot point with a comparatively weaker energy content. The refraction arrivals from the Moho region start to appear at 225 km from the shot point. The wave pattern has a very low frequency content and is perturbed severely by the ground noise. However, we were able to pick up the Pn arrivals from four geophone locations. The corresponding least square velocity is 8.12 km/sec. Continuation of this phase towards the corresponding reflection branch (PmP) could not be traced possibly because of its weak character. Considering the first arrivals from all the evident refractors we estimated their depths from the respective intercept times using either equation-7 or equation-8 thus getting our first rough model (model M1, figure-6.5) from the horizontal layer interpretation. We also computed the maximum and minimum bounds of depths using equations-4 & 6 in chapter-4. The computed results are included in table-6.2. From the table we see that the total thickness of the crust is 44.5 km under the study area. The estimated horizontal layer model lies within the limits of the maximum and minimum values. Apart from the observed discrepancy

TABLE:6.1 Comparison of results from well logs and seismic observation.

| parameters | well data | seismogram |
|---|---|---|
| (1) 2-way intercept time | 1.45 sec | 1.34 sec |
| (2) average velocity of sediments | 3.20 km/sec | 3.64 km/sec |
| (3) depth of basement | 2.66 km | 3.03 km |

TABLE:6.2 Nominal parameters as calculated for the Horizontal layer model.

| Layer | Velocity km/sec | Thickness km | Depth km | Min-Max depth km |
|---|---|---|---|---|
| 1 | 3.2 | 2.5 | 0.0 | 0.0- 0.0 |
| 2 | 6.0 | 2.5 | 2.5 | 2.5- 3.4 |
| 3 | 6.2 | 9.9 | 5.0 | 3.9- 5.2 |
| 4 | 6.5 | 5.4 | 14.9 | 13.0-16.5 |
| 5 | 6.7 | 24.2 | 20.3 | 19.0-24.5 |
| 6 | 8.1 | - | 44.5 | 40.8-54.0 |

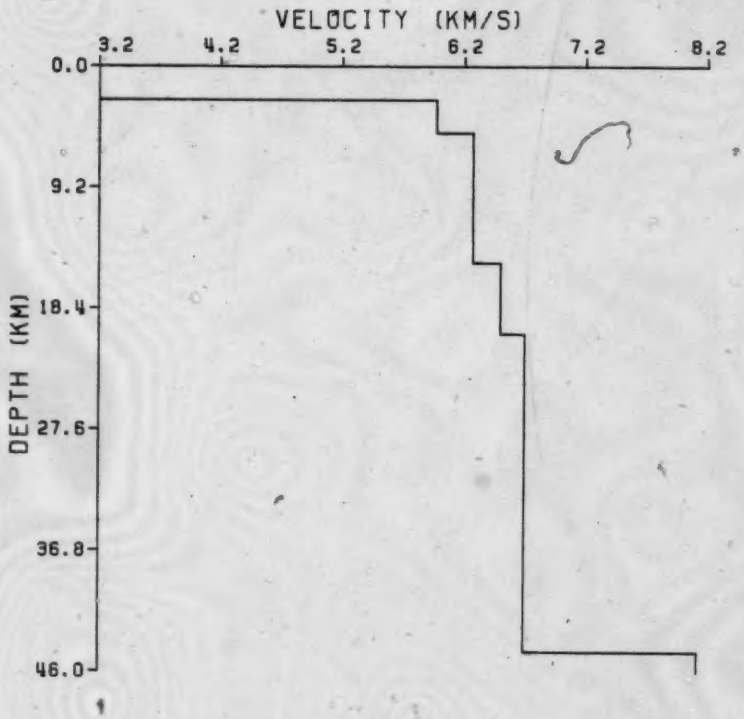


Figure 6.5 Model M1 from horizontal layer interpretation.

between theoretical and observed critical points of the PmP branch (132 and 152 kms respectively), the results from the horizontal layer model can be considered fairly convincing up to this point.

**6.2 WHB inversion:**

The plane layered interpretation from the first arrival data assumed constant velocities within each layer. This assumption is only an approximation to the more general case where velocity usually increases with depth due to overburden pressure (Birch, 1964). Therefore if we assume that the horizontal layer model (considering straight ray paths) gives only a minimum estimate of the depths, we must introduce another method which will give exact maximum depths. This method is the WHB inversion and is equivalent to the method of getting approximate upper limits of depths discussed in chapter-4.

All the first break times across the seismic section were approximated by a third order polynomial curve fitted in the least squares sense. All data were reduced to the base of the sedimentary layer before fitting. Then we differentiated this approximate function to estimate dT/dX as required by the integral equation-9 in chapter-4 and computed the corresponding depths. The integration was performed by using the Trapezoidal rule. The results obtained from this method were similar to the horizontal

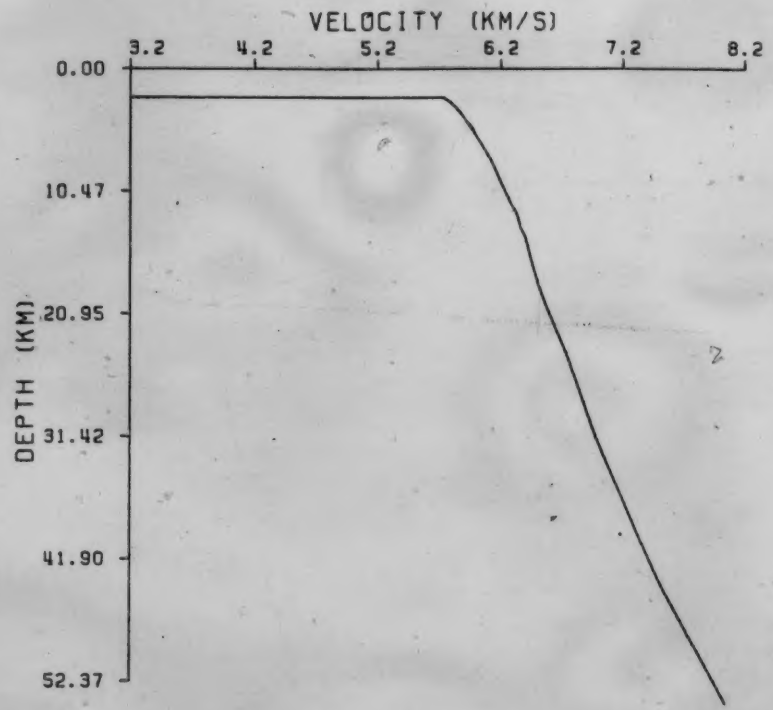


Figure 6.6 Model M2 from WHB inversion.

layer model except for the region of the lower crust. The depth of Moho obtained from the WHB method was 52 km whereas the one computed from horizontal layer interpretation was 44.5 km (table-6.2). The difference is presumably due to the effect of the gradual increase of velocity with depth in the WHB method. Therefore it is clear that the introduction of a velocity gradient in the lower crust will increase the depth of the Moho to an amount not exceeding 52 kilometers. The model M2 as derived from the WHB inversion is shown in figure-6.6.

**6.3 Analysis of reflection branches:**

One of the principal aims of this experiment was to record wide angle reflections. Indeed we recorded very prominent reflection arrivals. Both subcritical and supercritical branches were observed in the seismogram. The simplest $T^2$-$X^2$ method was used to analyse these arrivals. At the beginning of the processing work, the reflection branches were partly obscured due to high noise level even after a 4-15 Hertz bandpass filtering. We decided to suppress the low frequencies and give preference to the comparatively high frequency reflections. With a band width of 6-13 Hertz the reflection arrivals became fairly easy to observe (figure-5.5, chapter-5). A group correlation method was applied to pick the reflection branches. The $T^2$-$X^2$ method established six wide angle branches with

corresponding depths at 11, 13.7, 19.5, 24, 27 and 43.4 kilometers (table-6.3). The interval velocities were computed from the Dix formula (equation-11, Chapter-4). Following Giese (1976) a correction of 10% & 3% for the computed depths and velocities were applied for the wide angle branches. Since correlation of secondary events involve the risk of large errors we did not intend to include these computed values in our final model. Rather we used them as an aid to a qualitative interpretation justifying the presence of the reflectors in the crust. The reflectors at 13.7, 19.5 and 43.4 kilometers correspond to the refractors mentioned in section-6.2 at similar depths as determined by the horizontal layer model (see table-6.2). The reflector at 24 km of depth does not appear as a refractor. This is due to a velocity inversion at this depth (see computed interval velocities in table-6.3) and hence would not be observed in the head wave data. The interface at 27 km however should refract seismic rays, since it apparently represents an increase in velocity as determined by interval velocity calculation. There is no clear explanation for the apparent absence of this refracted phase in the observed seismogram. Moreover the observed reflection branch corresponding to 24 km depth was so prominent that we could not ignore it or take it as a multiple reflection. It is possible that the weak refraction arrivals from the 27 km interface were obscured due to the low signal to noise ratio beyond 200 km. Another

TABLE:6.3 Results from $T^2$-$X^2$ analysis

| Layer | Interval velocity km/sec | Depth km | Min-Max depth km |
|---|---|---|---|
| 1 | 5.9 | 00.0 | 00.0-00.0 |
| 2 | 6.4 | 13.7 | 12.6-16.7 |
| 3 | 6.6 | 19.5 | 19.5-24.0 |
| 4 | 5.9 | 24.0 | 23.7-28.7 |
| 5 | 6.7 | 27.4 | 27.0-32.5 |
| 6 | 8.1 | 43.4 | 42.0-49.0 |

possible explanation requires a gradient zone between depths of 24 and 43.4 kilometers so that a head wave from 27 kms of depth is no longer possible, instead a retrogade branch is generated by the corresponding diving waves. For the later case the layered model in the lower crust will be only an approximation to the real situation. The crustal model obtained from the $T^2$-$X^2$ method (model M3) is plotted in figure-6.7. The average velocity of the crust (6.39 km/sec) obtained from this method is in good agreement with previous results (Sereda, 1978; p.193). We also computed the upper and lower bounds of the depth values for the reflection branches using equations-2 & 5 from chapter-4. The result is included in table-6.3. It is interesting to note that the calculated minimum values are almost equal to the $T^2$-$X^2$ results. This implies that these two methods are equivalent to each other. This also means that the $T^2$-$X^2$ method will always give a minimum estimation of the depth values. Although the computed depth and interval velocities were used as a diagnostic means to support the low velocity and the reflection branches, the exact values will be fixed by the synthetic modelling technique described below.

**6.4 Synthetic modelling:**

Interpretation was carried out by model calculation using the synthetic seismogram formulation described by Chapman (1978). The first model obtained from the direct

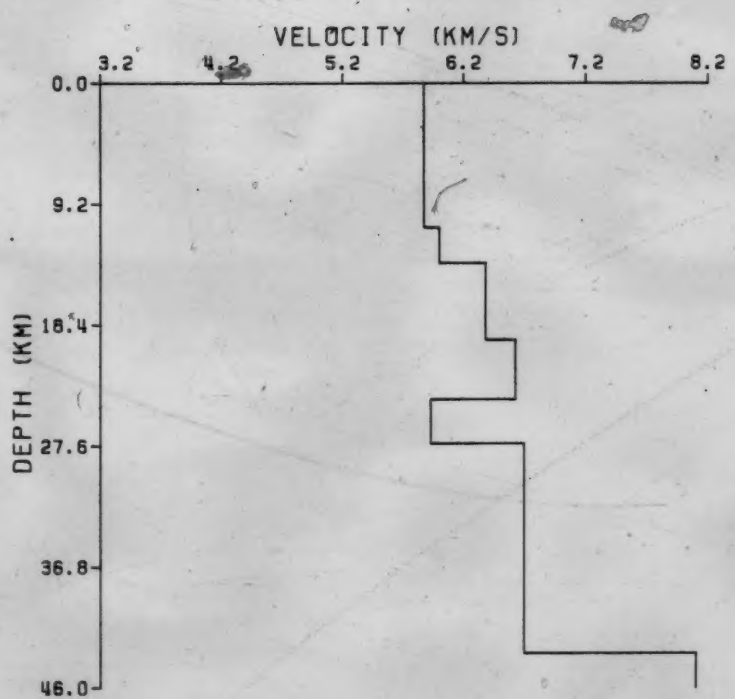


Figure 6.7 Model M3 from $T^2$-$X^2$ analysis.

inversion can be used as an input for the synthetic seismogram. Usually the synthetic obtained from the first model does not fit every feature of the observed data. Therefore one then tries to fit between the calculated and the observed travel times by changing the first model in a systematic way. By a trial and error process one can eventually reach a good agreement. We did not have a sure strategy for changing the model in a certain direction to reach better and better results, but we did find that by applying few changes at once and starting from the surface downwards one obtains results most quickly. In any case uniqueness will always remain questionable. By using a trial and error method in changing the models one finds that one is always pushed in a certain direction, that is, independent of the type of model one starts with, one will end up with a particular class of model. This however does not imply that the final model will truely represent the actual conditions; it will still be a model albeit a fairly good one.

Densities for the input model were computed from (Birch, 1964)

$$\rho = 0.252+0.3788Vp$$

and the shear wave velocities were calculated from the corresponding P-wave values by assuming the Poisson's ratio equal to 0.25. Attenuation factors were not considered for

computing the amplitudes. The synthetic obtained from the input model M1 from horizontal layer calculations is shown in figure-6.8. It is clear that the first arrivals are successfully reproduced by the synthetic. The Pn arrivals are very weak and the maximum amplitude for PmP lies at 140 km which according to our previous calculation should be 132 km. Also it does not reproduce all the reflection branches that we identified on the observed seismogram. Considering the results from the $T^2$-$X^2$ interpretation we then introduced two low velocity zones at 11-14 and 24-27 kilometers of depths. Most of the features were in good agreement except that the PmP branch was much earlier than is required by the data. Adjusting the low velocity zone at 24-27 km allowed us to fix this very easily. This led to a critical distance closer to the shot point (figure-6.9) and was an additional advantage of the new model, since this agrees better with the observations. Actually the position of the maximum amplitude of the PmP branch depends on the frequency content of the corresponding signals. According to Cerveny (1966) the critical point for a 6 Hertz signal reflected from the Moho interface usually lies at about 10-25 km beyond the theoretical value. Therefore observed and theoretical critical distances of 152 and 132 kms for the PmP are clearly admissible. The new model is shown in figure-6.10 and will be called the model M4 hereafter. Table-6.4 contains the adjusted parameters for the model M4. A ray diagram corresponding to model M4 is shown in figure-6.11.

TABLE:6.4 Nominal parameters as calculated for the final model (M4).

| Layer | Velocity km/sec | Thickness km | Depth km |
|---|---|---|---|
| 1 | 3.2 | 2.8 | 0.0 |
| 2 | 6.0 | 2.3 | 2.8 |
| 3 | 6.2 | 6.0 | 5.0 |
| 4 | 6.1 | 3.0 | 11.0 |
| 5 | 6.5 | 5.0 | 14.0 |
| 6 | 6.7 | 6.0 | 19.0 |
| 7 | 6.1 | 4.0 | 25.0 |
| 8 | 6.7 | 15.5 | 29.0 |
| 9 | 8.1 | - | 44.5 |

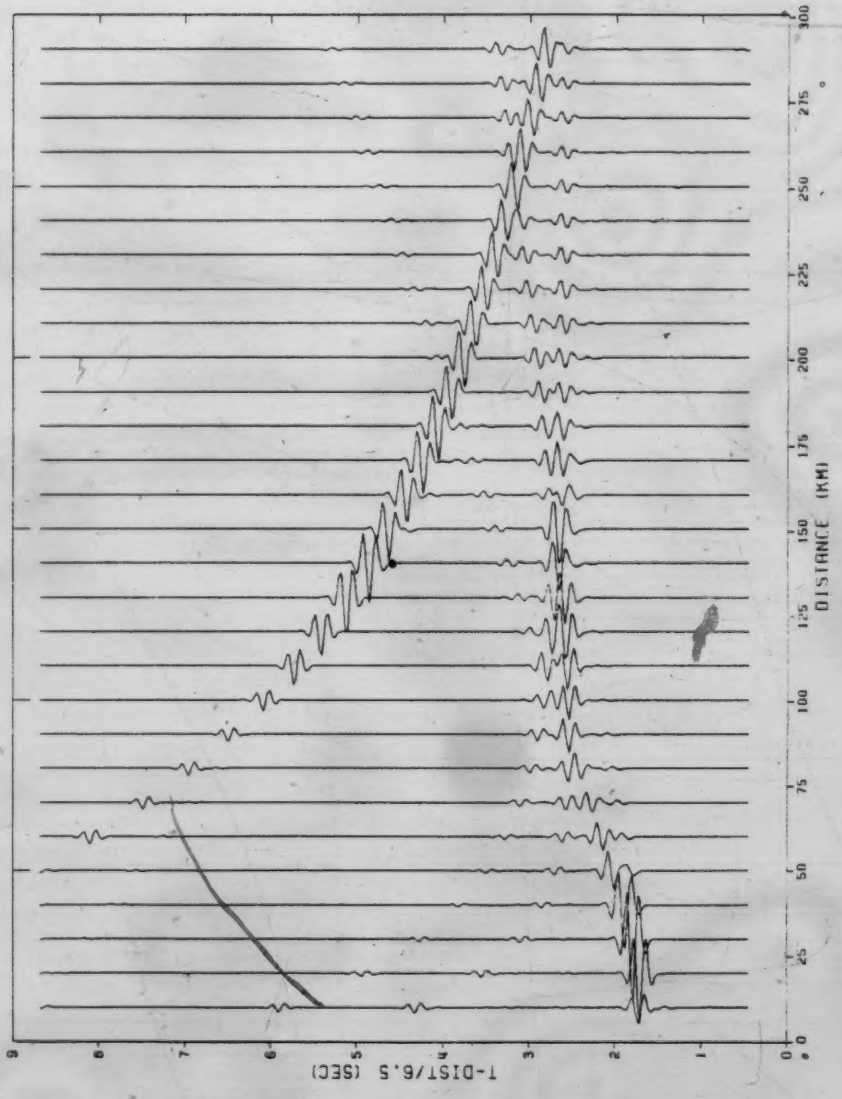


Figure 6.8 Synthetic seismogram obtained from model M1 of horizontal layer interpretation (a dot on the PmP indicates the position of the maximum amplitude).

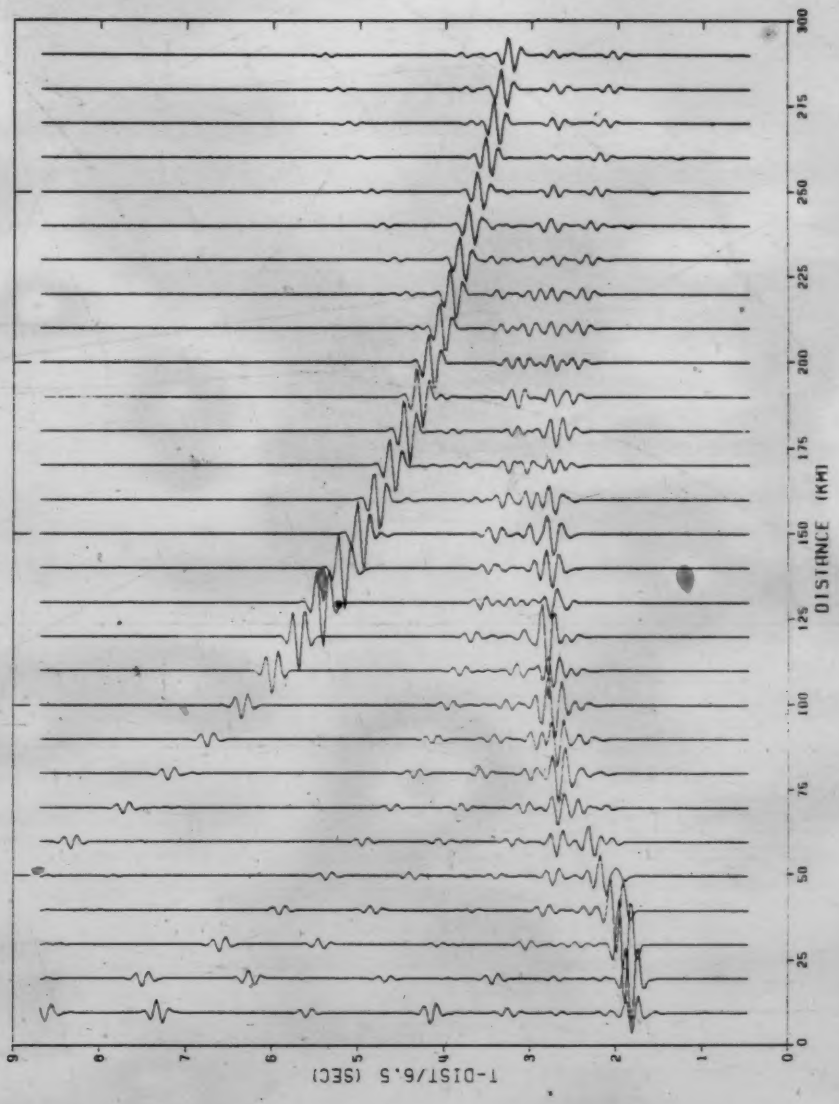


Figure 6.9 Synthetic seismogram from the final model M4 (a dot on the PmP indicates the position of the maximum amplitude).

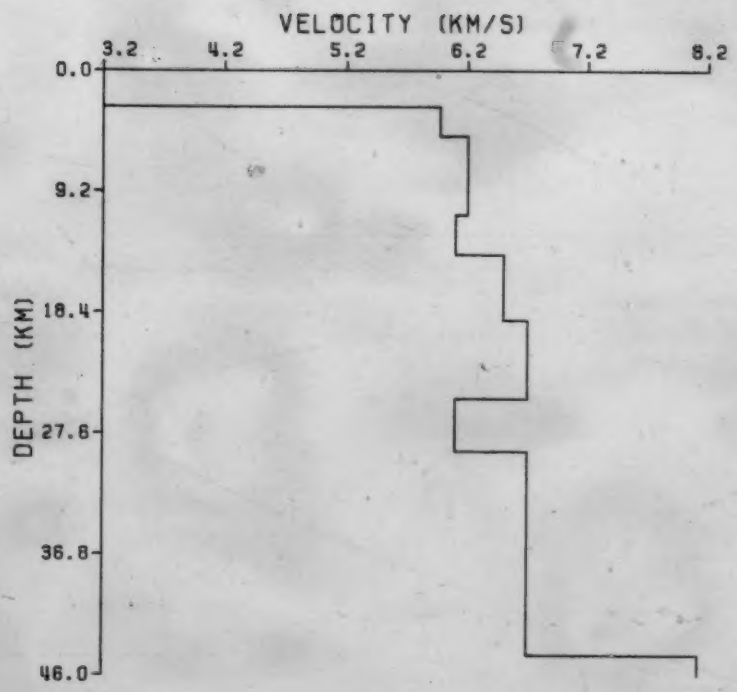


Figure 6.10 Final model (M4) showing the crustal stucture under the study area.

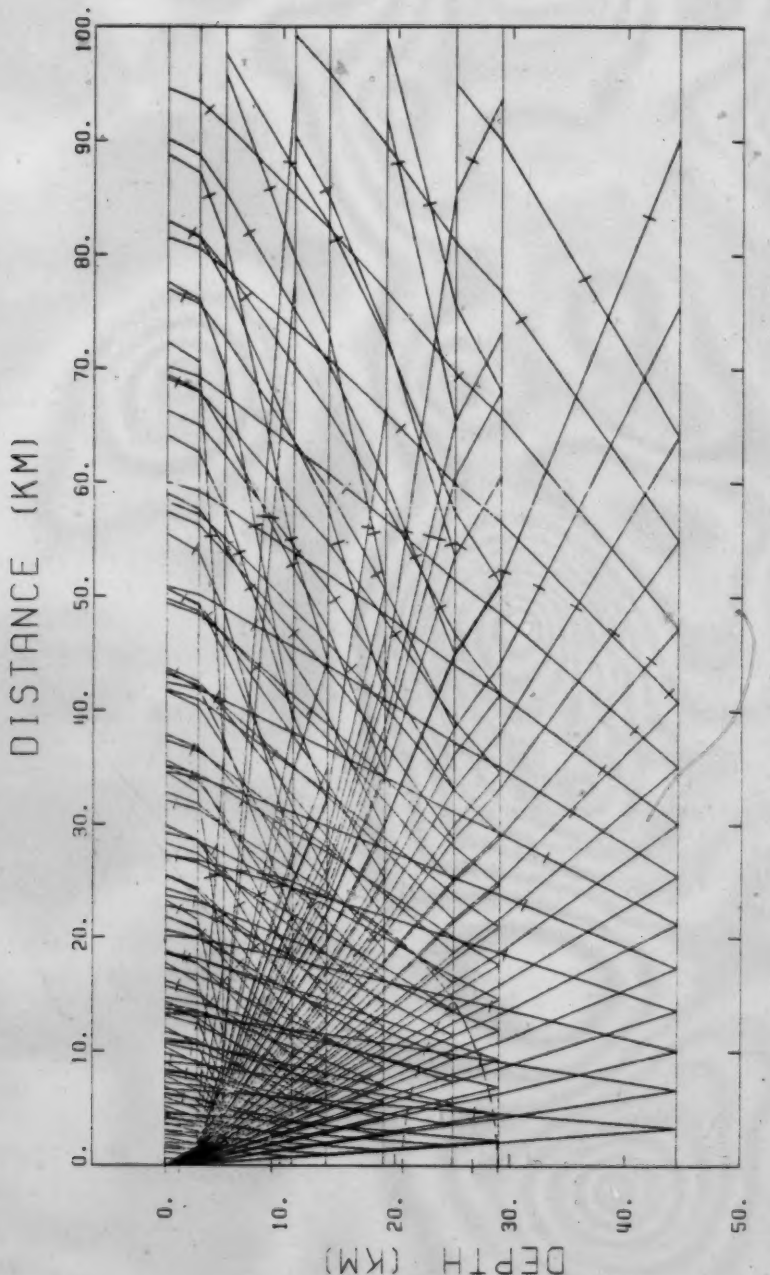


Figure 6.11 Ray diagram corresponding to the final model (M4). Dashed curves represent the wave fronts.

We consider model M4 as our final presentation of the crustal structure under the study area. Of course some of the features remain quite speculative. This is a limitation we could not avoid due to the lack of a reversed profile and the difficulties associated with obtaining amplitude information.

## 7. DISCUSSION

In the last chapter interpretation of the observed data were carried out on the basis of first and reflected arrivals, critical points and approximate relative amplitudes. It is also worthwhile to discuss the derived crustal model in terms of the tectonic history of the region, the lithology at various depths and if possible the physical parameters such as pressure, temperature, conductivity, porosity etc as a function of depth.

Variation of the seismic velocities with depth in the crust can be related to the changes in gross chemical composition and/or progressive metamorphism. Many geo-scientists consider that generally the earth's crust consists of an upper crystalline basement composed of metamorphic rocks such as gneisses and schists, an intermediate zone of migmatites and the lower crust of granulite facies rocks. The observed rapid velocity increase from 5.97 to 6.2 km/sec in the basement rocks may correspond to a gradient zone with increasing closure of microfractures due to overburden pressure. Beneath this gradient zone, the velocity becomes nearly constant at 6.49 km/sec. This fact is consistent with the behavior of either dry or saturated rocks subjected to increasing confining pressure, pore pressure being low. The next layer of 6.7 km/sec velocity is a similar zone with a difference in chemical composition and/or gradational metamorphism. Crustal velocities of the order of 6.0 km/sec are

interpreted as an indication of granitic rocks while those with more than 7.0 km/sec are assumed to be of gabbroic composition. A velocity of 6.7 km/sec in the middle and lower crust therefore, should correspond to a layer of intermediate composition. The low velocity in the lower part of the basement was suggested by several factors:

(1) rapid attenuation of the Pg branch after 70 km.

(2) observed reflection branch from a possible interface at 11 km depth.

(3) observed high amplitude of the refracted/reflected signals from the top of the 6.49 km/sec layer.

(4) observed critical point much smaller than the calculated one for the reflection branch from the top of the 6.49 km/sec layer (theoretical and observed values are 109 & 90 kms respectively).

A low velocity zone at the lower basement may be explained as due to an intrusive sheet and possibly relates to a high conductive region in the crust as proposed by Camfield and Gough (1977). From figure-2.4 it appears that the NACP anomally is located approximately between longitudes 104.5°W and 105.5°W at latitude 49°N. This means that normally we should expect to see any seismic expression of the anomally within 50-105 km from the shot point. From the observed seismogram we find that a rapid attenuation of the Pg amplitudes occur between 65 and 100 kilometers from the shot. This suggests that there may be an inhomogeneous structure present in the crust under the basement. From the

interpretation of these attenuated and delayed phases we proposed a low velocity structure under the 6.2 km/sec layer (section-6.1). If we want to relate this velocity low to the NACP anomally the following discrepancies arise:

(1) In north Saskatchewan, the narrow conductive anomally was shown to be associated with steeply dipping graphite sheets, which means a near vertical structure of the conductive body. The low velocity zone obtained from this study was only a thin horizontally layered structure.

(2) the NACP body was proposed to be at the surface of the Precambrian. The present study indicated a low velocity zone just below the basement layer.

(3) suggested velocity for the low velocity zone was of the order of 6.1 km/sec from this study whereas the conductive materials of Camfield and Gough were thought to be graphitic sheets having a much lower velocity.

However the following points are also important:

(1) the low velocity zone was indicated by the anomally in the data just at the region where the NACP anomally was expected.

(2) the depth of the conductive body at a particular location does not necessarily imply that it will have the same depth at other locations.

In fact the NACP body was shown to have different depths between 3 and 75 km at different locations of North America. Therefore a slightly greater depth of the conductive body at the study area is clearly admissible and

we can conclude that the observed low velocity below the 6.2 km/sec layer might correspond to the same conductive body as proposed by Camfield and Gough.

The velocity inversion at 25-29 km depth is more well developed and is suggested by the computed interval velocities from $T^2$-$X^2$ analysis. The velocity low at this depth could also be related to high conductivity, as mentioned by Sternberg and Clay (1977), Barry et al (1977) and Chaipayungpun and Landisman (1977). The existence of a low velocity layer in the middle crust can be related to concentrated waters in the first formed granitic melts. It is quite possible that this 'wet zone' may have a velocity lower than the material above and even lower than the dehydrated material below (Berry, 1972). The release of free water into the surrounding pore spaces would provide a consistent explanation for the lowered seismic velocities, the increase of attenuation, the reduction of cohesive strength and also the higher electrical conductivity in the crust.

For simplicity we took the crust-Moho transition to be a first order discontinuity, but we did not rule out the possibility of a broader transition zone at this region. The observed characteristics such as long duration of the signals, high amplitude reflection arrivals and the splitting of the PmP reflections may suggest a complex layering of alternate low and high velocities (Fuchs, 1969; Clowes & Kanasewich, 1970; Giese 1976). Moreover numerical

experiments indicated that the only effective way to increase the apparent time duration of the reflected energy is to increase the thickness of the transition zone.

Considerable effort was spent in attempting to find other models that would explain all the main features of the observed seismogram. All such efforts were unsuccessful. Therefore we suppose that the model presented in this study is a reasonable representation of the crust as illuminated by a source and viewed along a line in one direction from the source. The result could be more authentic if we had at our disposal, data from a reversed profile along the same line of observation. Refraction studies from adjacent profiles indicated that apart from the local deviations the dip of the crustal layers hardly exceeds 3°, therefore true values of depths should not be significantly different from the calculated ones. In any event, the general structure of the layered crust should remain more or less the same.

We also compared the derived final model with the results of other refraction profiles close to the study area. Comparing to the Swift Current and Weyburn models in figure-2.7 we see that the upper crustal velocities are similar. A refractor having a velocity of 7.1 km/sec and depths of 36 and 41 kms respectively as identified at Suffield and Weyburn is not reflected in our data, instead we found a shallower layer with a velocity of 6.7 km/sec. It is possible that these two velocities have similar compositions with difference in densities. It was proposed

that (Green et al, 1979) a crustal fault at 103°W is responsible for the differences in Moho depths on either side of it. Therefore even without the knowledge of the correct position of the fault we could possibly explain the variation of the Moho depths at Weyburn and Limerick as due to this fault. The difference between Moho depths at Swift current and Limerick (about 2.0 km) is small and can be associated with a small dip. It again proves that the thickness of the crust does not vary too much at these two localities.

Figures 7.1 & 7.2 show the interpreted results from the 1979 north-south and 1977 east-west refraction profiles. The depths and velocities of the refractors obtained from our study is supported by these results. The results obtained from the 1979 north-south profiles are similar to the ones obtained from this study only for the upper and middle crust. An increase of moho depth by 3 km towards the south can be related to the Williston Basin tectonics. Comparison of the refraction results as a whole indicated that:

(1) our profile lies entirely within the Churchill province.
(2) the simple layered model of the crust is well suited for this area.
(3) the structure is more or less homogeneous in the vertical direction.

The position of the 103°W fault could not be identified from our data since the profile does not really cover the

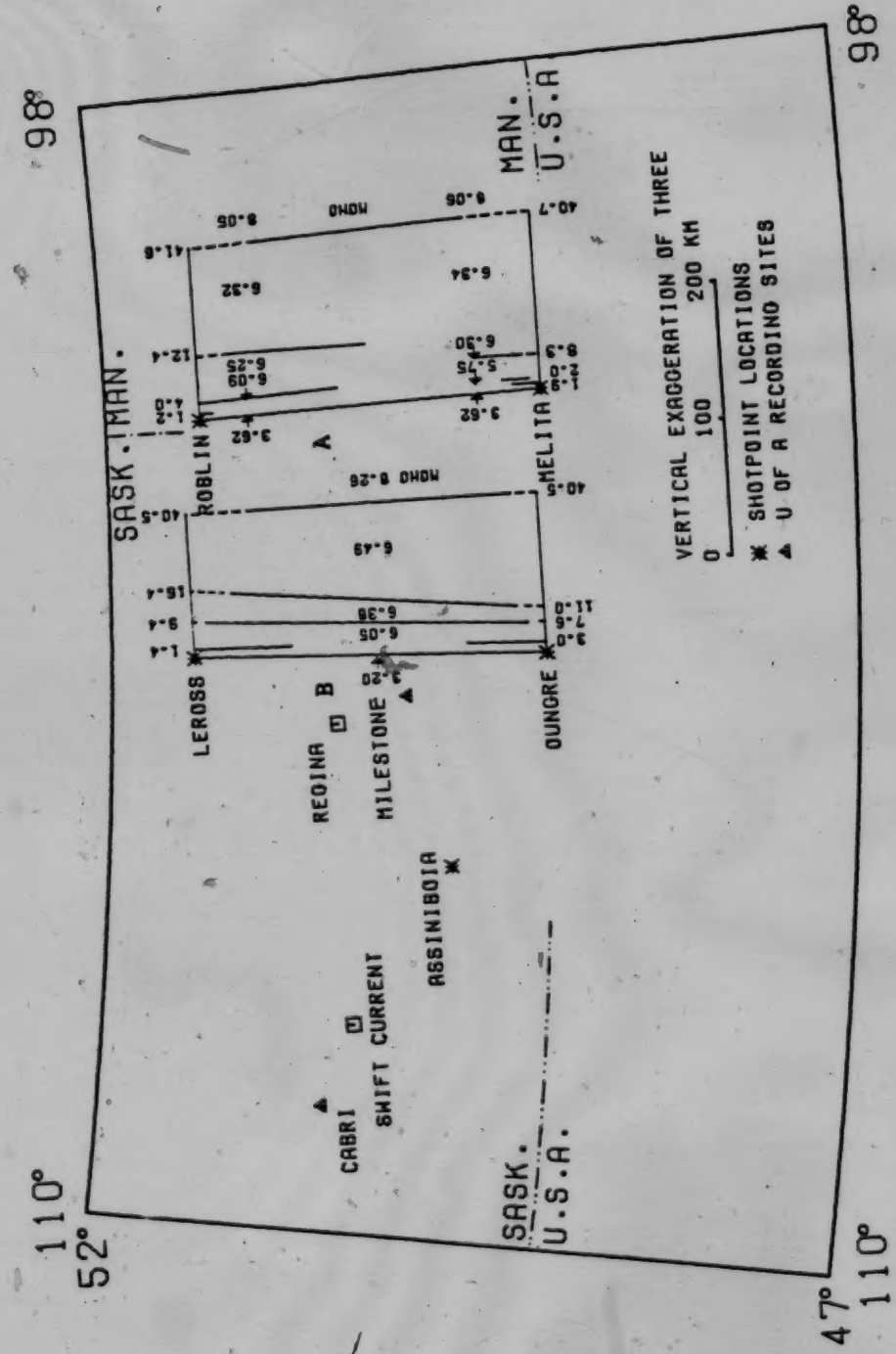


Figure 7.1 Crustal models from CO-CRUST 1979 refraction experiment (after Sprenke, 1982).

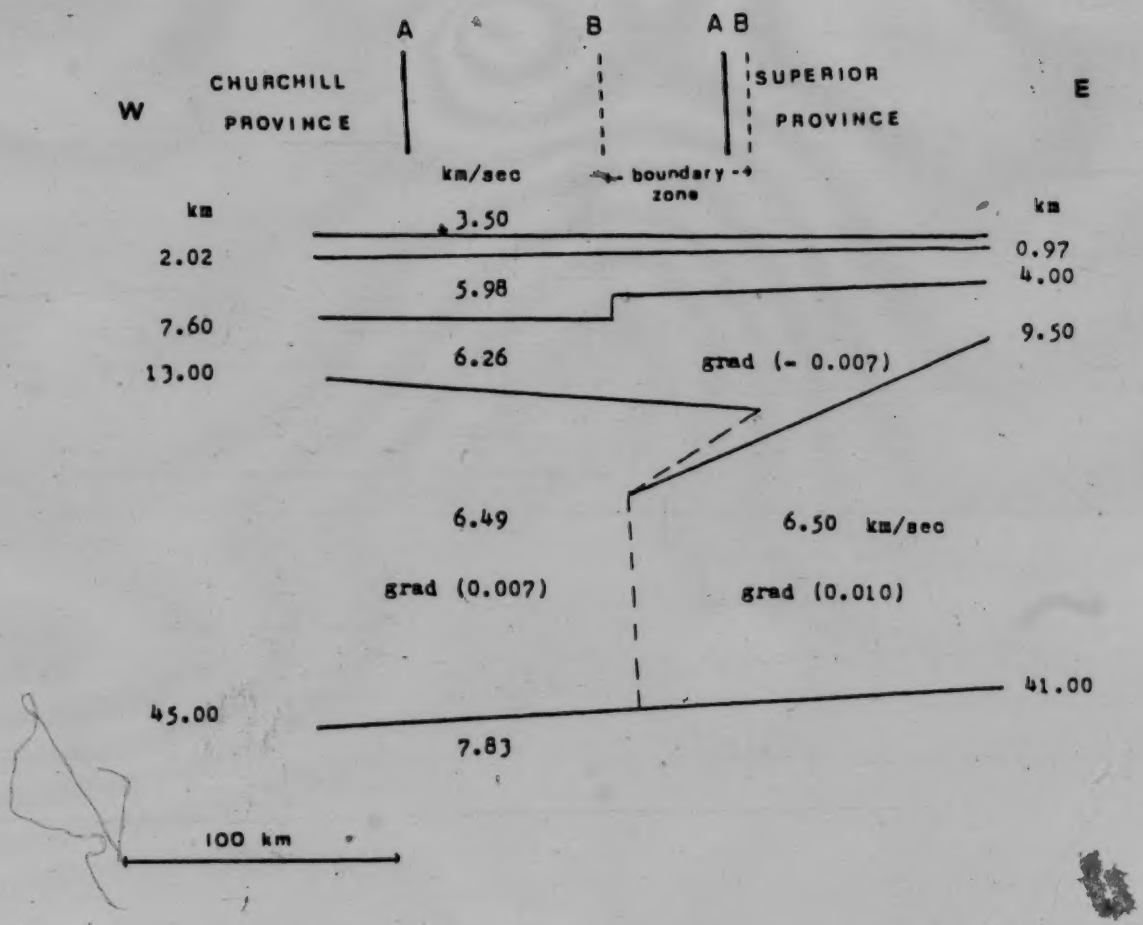


Figure 7.2 Crustal model from CO-CRUST 1977 east-west refraction profile (after Moon and de Landro, 1981).

fault area (figure-1.1). However combining the results of this study and the ones from the 1977 east-west profile (Moon and de Landro, 1981) indicates that the position of the fault should be somewhat to the east of longitude 103°W. Determination of the exact position of the fault may be possible by a near vertical reflection experiment in an area between longitudes 103°W and 100°W near the international border.

Due to inadequate control over the seismometer gains we had difficulties in interpreting the dynamic characteristics of the waves. Therefore we recommend that more care should be taken in future to retain the amplitude information. To achieve a reasonable control over the sedimentary velocity, more detectors should be placed within 15 kilometers of the shot point.

## BIBLIOGRAPHY


Barry, R. Lienert and Bennett, D. J. 1977. High electrical conductivities in the lower crust of Northwestern Basin and Range: An application of inverse theory to a controlled source deep magnetic sounding experiment, The Earth's crust, Geophys. Monogr. Ser. Vol.20, edited By J. G. Heacock AGU, Washington, D. C., pp. 531-552.

Bateman, H. 1910. The solution of the integral equation connecting the velocity of propagation of an earthquake wave in the interior of the earth with the times which the disturbance takes to travel to the different stations on the earth's surface, Phil. Mag., 19, pp. 576-587.

Bell, C. K. 1971. History of the Superior-Churchill Bounday in Manitoba, Geological Association of Canada, Special paper, v.9, pp. 5-39.

Berry, M. J. 1971. Depth uncertainties from seismic first arrival refraction studies, J. Geophys. Res., 76, p. 6464.

_____, 1972. Low velocity channels in the earth's crust, Comments Earth Sci., Geophysics, 3, pp. 59-68.

_____, and Mair, J. A. 1977. The nature of the earth's crust in Canada, The Earth's crust, Geophys. monogr. Series., vol.20, edited by J. G. Heacock AGU, Washington, D. C., pp. 318- 348.

Birch, F. 1964. Density and composition of the mantle and core, J. Geophys. Res., 69, pp. 4377-4387.

Braile, L. W. and Smith, R. B. 1975. Guide to the interpretation of crustal refraction profiles, Geophys. J. R. Astr. Soc., 40, pp. 145-176.

Burwash, R. A. and Culbert, R. R. 1976. Multivariate

geochemical and mineral patterns in the Precambrian basement of western Canada, Canadian Journal of Earth Sciences, vol.13, pp. 1-18.

Camfield, P. A. and Gough, D. I. 1977. A possible Proterozoic plate boundary in North America, Canadian Journal of Earth Sciences, vol.14, pp. 1229-1238.

Cerveny, V. 1966. On dynamic properties of reflected and head waves in the n-layerd earth's crust, Geophys. J. R. Astr. Soc., 11, pp. 139-147.

Chaipayungpun, W. and Landisman, M. 1977. Crust and upper mantle near the western edge of the great plains, The Earth's crust, Geophys. Monogr. Ser., vol.20, edited by J. G. Heacok, AGU, Washington, D.C., pp. 553-575.

Chandra, N. N. and Cumming, G. L. 1972. Seismic refraction studies in Western Canada, Canadian J. of Earth Sciences, 9, p. 1099.

Chapman, C. H. 1978. A new method for computing synthetic seismogram, Geophys. J. R. Astr. Soc., 54, pp. 481- 518.

Chiu, S. K. 1982. Crustal structure beneath Vancouver Island from refraction data, M.Sc. thesis, University of Alberta, Edmonton, Alberta, Canada., pp. 29-37.

Clowes, R. M. and Kanasewich, E. R. 1970. Seismic attenuation and the nature of the reflecting horizons within the crust, J. Geophys. Res. 75, pp. 6693-6705.

Cormier, V. F. and Richards, P. G. 1977. Full wave theory applied to a discontinuous velocity increase: the inner core boundary, J. Geophys., 43, pp. 3-31.

Cumming, G. L. and Kanasewich, E. R., 1966. Crustal structure in western Canada, Report period ending June 30, 1966, Work sponsored by Advanced

Research Projects Agency and Defense Research Board of Canada.

Dey-Sarker, S. K. and Chapman, C. H. 1978. A Simple method for the computation of body wave seismograms. Bull. Seis. Soc. Am., vol.68, no.6, pp. 1577-1593.

Dix, C. H. 1955. Seismic velocities from surface measurements, Geophysics, 20, pp. 17-26.

Dobrin, M. B. 1976. Introduction to geophysical prospecting, 3rd edition, McGraw Hill, Toronto, Ontario, p. 137.

Douglas, R. J. W. 1970. Geology and Economic Minerals of Canada.

Fuchs, K. 1969. On the properties of deep crustal reflectors, Z. Geophys., 35, pp. 133-149.

_____, and Muller, G. 1971. Computation of synthetic seismograms with the reflectivity method & comparison with observation, Geophys. J., 23, pp. 417-433.

Gerver, M. and Markushevich, V. 1967. On the characteristic properties of travel time curves, Geophys. J. R. Astr. Soc., 13, pp. 241-246.

Giese, P. 1976. Calculation of depths, Explosion Seismology in Central Euorope-Data and Results, edited by P. Giese, C. Prodehl and A. Stein, Springer, New York, pp. 146-161.

_____, 1976a. Models of crustal structure and main wave groups, Explosion Seismology in Central Europe-Data and Results, edited by P. Giese, C. Prodehl, and A. Stein, Springer, New York, p. 196.

Grant, F. S. and West, G. F. 1965. Interpretation theory in applied geophysics, McGraw Hill company, New York.

Green, A. G., Cumming, G. L. and Cedarwell, D. 1979. The Superior-Churchill boundary zone in southern Canada, Center for Precambrian Studies Publication no.34, University of Manitoba, Winnipeg, Canada.

_____, and Stephenson, D. G. 1977. Cooperative near vertical incident reflection and refraction/wide angle reflection seismic surveys across Superior-Churchill boundary zone in southern Canada, Part 1, A technical report.

Gutenberg, B. 1955. Channel waves in the earth's crust, Geophysics, 20, pp. 283-294.

Hall, D. H. and Brisbin, W. C. 1965. Crustal structure from converted head waves in Central Western Manitoba, Geophysics, 30, pp. 1053-1067.

_____, and Hajnal, Z. 1973. Deep crustal studies in Manitoba, Bull. Seis. Soc. Am., vol.63, pp. 885-910.

Hajnal, Z. and Rose, T. C. 1979. A quantitative correlation of seismic, gravity and tectonic models along the Nelson Front, (manuscript)

_____, 1981. The second phase of CO-CRUST seismic project in southern Canada. Earth Physics Branch Open File report No.81.

Herglotz, G. 1907. Uber das Bennderfsche Problem der Fortpflanzungsgeschwindigkeit der Erdbebenstrahlen, Phys. Z., 8, pp. 145-147.

Kanasewich, E. R., Clows, R. M. and McClougham, C. H. 1969. A burried Precambrian rift in Western Canada, Tectophysics, 8, pp. 513-527.

_____, 1975. Time sequence analysis in geophysics, 2nd edition, University of Alberta press, Edmonton, Alberta, Canada, pp. 64-72.

Kazmierczak, Z. 1980. Seismic crustal studies in

Saskatchewan, M.Sc. thesis, University of Alberta, Edmonton, Alberta, Canada. pp. 64-77.

Kornik, L. J. and Maclaren, A. S. 1966. Aeromagnetic study of the Churchill-Superior boundary in northern Manitoba, Canadian Journal of Earth Sciences, vol.3, pp. 547-557.

Landisman, M., Mueller, S. and Mitchell, B. J. 1971. Review of inversions in the earth's crust., Geophys. Monogr. Ser. vol.14, edited by J. G. Heacock. Washington, D. C., p. 11.

Lee, S. K. J. 1977. Multilayer gravity inversion using Fourier transform, M. Sc. thesis, University of Alberta, Canada, p. 141.

Maureau, G. T. 1964. Crustal structure in western Canada, M.Sc. thesis, University of Alberta, Canada.

Mitchell, B. J. and Landisman, M. 1971. Geophysical measurement in the Southern Great plains, Geophys. Monogr. Ser., vol.14, pp. 77-93.

Moon, W. and de Landro, W. 1981. Detailed interpretation of CO-CRUST 1977 refraction data, Publication of the Center for Precambrian Studies, University of Manitoba, Winnipeg, Canada.

Mueller, S. 1977. A new model of the continental crust, Geophys. Monogr. Ser., vol.20, edited by J. G. Heacock, AGU, Washington, D. C., pp. 289-317.

Pavlenkova, N. I. 1968. Methods of velocity determination from seismic crustal studies, Conference of experts on explosion seismology, Leningrad, USSR.

Richards, T. C. and Walker, D. J. 1959. Measurements of the thickness of the earth's crust in the Albertan plains of Western Canada, Geophysics, 24, pp. 262-284.

Sereda, I. V. 1978. A crustal reflection expanding spread study in southeast Saskatchewan and southwest Manitoba, M.Sc. thesis, University of Saskatchewan, Saskatoon, Canada.

Slichter, L. B. 1932. The theory of the interpretation of travel time curves in horizontal structures, Physics, 3, pp. 273-295.

Sprenké, K. F. 1982. Potential field inversion, Ph.D. thesis, University of Alberta, Edmonton, Alberta., Canada.

Steinhart, J. S. and Meyer, R. P. 1961. Explosion studies of continental structure, Carnegie Institution of Washington, publication-622, Washington, D. C., pp. 305-340.

Sternberg, B. K. and Clay, C. S. 1977. Flambeau anomally: A high conductivity anomally in the southern extension of the Canadian shield, The Earth's crust, Geophys. Monogr. Ser. , vol.20, edited by J. G. Heacock, AGU, Washington, D. C., pp. 501-530.

Stewart, S. W. 1966. Seismic ray theory applied to refraction surveys of the earth's crust in Missouri, Ph.D. thesis, St. Louis University, St. Louis, Missouri, USA, p. 189.

Telford, W. M., Geldart, L. P., Sheriff, R. E. and Keys, D. A. 1976. Applied geophysics, Cambridge University press, Cambridge, London.

Van Zijl, J. S. V. 1977. Electrical studies of the deep crust in various tectonic provinces of southern Africa, in the Earth's crust: its nature of physical properties, Geophys. Monogr. Ser., vol.20, edited by J. G. Heacock, AGU. Washington., D. C., pp. 470-500.

Weaver, D. 1962. Crustal thickness in southern Alberta, M.Sc. thesis, University of Alberta, Canada.

Wiechert, E. 1910. Bestimmung des weges der Erdbebenwellen im Erdinnern, 1. Theoretisches., Phys. Z., 11,

pp. 294-304.

Wiggins, R. A. and Helmberger, D. U. 1973. Upper mantle structure of the western United States, J. Geophys. Res., 78, pp. 1870-1880.

_____, and Madrid, J. A. 1974. Body wave amplitude calculations, Geophys. J., 37, pp. 423-433.

_____, 1976. Body wave amplitude calculations-II, Geophys. J., 46, pp. 1-10.